Kinematic Analysis of Multi-DOF Planar Mechanisms via Velocity-Coefficient Vectors and Acceleration-Coefficient Jacobians

Raffaele Di Gregorio

Department of Engineering, University of Ferrara
Via Saragat,1; 44122 FERRARA; Italy
T: +39-0532-974828, F: +39-0532-974870
E: raffaele.digregorio@unife.it

Abstract

In the literature, velocity coefficients (VCs) and acceleration coefficients (ACs) were substantially proposed for single-degree-of-freedom (single-DOF) planar mechanisms. Their effectiveness in solving the kinematic analysis of these mechanisms is due to the fact that they only depend on the mechanism configuration. Such property also holds when they are defined for spatial single-DOF scleronomic and holonomic mechanisms, but was not exploited; moreover, some extensions of the VC and AC concepts to multi-DOF planar (or spatial scleronomic and holonomic) mechanisms are possible, but have not proved their practical usefulness. Here, first, the velocity-coefficient vectors (VCVs) together with their Jacobians (acceleration-coefficient Jacobians (ACJs)) are proposed as an extension of the concepts of VC and AC to multi-DOF scleronomic and holonomic mechanisms. Then, a general algorithm, based on VCVs and ACJs and on a notation, previously presented by the author, which uses the complex-number method, is proposed for solving the kinematic-analysis problems of multi-DOF planar mechanisms and to find their links' dead-center positions. The effectiveness of the proposed algorithm is also illustrated by applying it to a case study. The proposed algorithm is efficient enough for constituting the kinematic block of any dynamic model of these mechanisms, and simple enough for being presented in graduate courses.

NOMECLATURE:
DOF = degrees of freedom
VC = velocity coefficient
AC = acceleration coefficient
VCV = velocity-coefficient vector
ACJ = acceleration-coefficient Jacobian
m = number of mechanism's links
a = number of mechanism's independent loops
f = DOF number
e = number of secondary variables
ξ_j = j-th generalized coordinate, $j \in \{1,\ldots,f\}$
$\boldsymbol{\xi} = (\xi_1, \ldots, \xi_f)^T$
ζ_i = i-th secondary variable, $i \in \{1,\ldots,e\}$
$\nu_{ik,} = \dfrac{\partial \zeta_i}{\partial \xi_k}$, $i \in \{1,\ldots,e\}$ and $k \in \{1,\ldots,f\}$
$\mathbf{v}_i = (\nu_{i1}, \ldots, \nu_{if})^T$
$$\boldsymbol{\Lambda}_i = \begin{bmatrix} \dfrac{\partial \nu_{i1}}{\partial \xi_1} & \cdots & \dfrac{\partial \nu_{i1}}{\partial \xi_f} \\ \vdots & \ddots & \vdots \\ \dfrac{\partial \nu_{if}}{\partial \xi_1} & \cdots & \dfrac{\partial \nu_{if}}{\partial \xi_f} \end{bmatrix}$$
$\mathbf{z}_{kj}$ = complex number associated to the k-th edge of the j-th loop
θ_k = angle that gives the orientation of the k-th link with respect to the frame
d_s = joint variable of a prismatic (P) pair
$\boldsymbol{\delta}_s = \nabla d_s$

$$\mathbf{\Delta}_s = \begin{bmatrix} \dfrac{\partial \delta_{s1}}{\partial \xi_1} & \cdots & \dfrac{\partial \delta_{s1}}{\partial \xi_f} \\ \vdots & \ddots & \vdots \\ \dfrac{\partial \delta_{sf}}{\partial \xi_1} & \cdots & \dfrac{\partial \delta_{sf}}{\partial \xi_f} \end{bmatrix}$$

ψ_{kr} = curve parameter of a conjugate profile fixed to a link

$\boldsymbol{\varepsilon}_{kr} = \nabla \psi_{kr}$

$$\mathbf{\Gamma}_{kr} = \begin{bmatrix} \dfrac{\partial \varepsilon_{kr1}}{\partial \xi_1} & \cdots & \dfrac{\partial \varepsilon_{kr1}}{\partial \xi_f} \\ \vdots & \ddots & \vdots \\ \dfrac{\partial \varepsilon_{krf}}{\partial \xi_1} & \cdots & \dfrac{\partial \varepsilon_{krf}}{\partial \xi_f} \end{bmatrix}$$

$\mathbf{v}_{B|g}$ = velocity, with respect to the frame, of a point B fixed to the g-th link

$\mathbf{a}_{B|g}$ = acceleration, with respect to the frame, of a point B fixed to the g-th link

1. Introduction

Standardized procedures for reducing the kinematic analysis of a generic planar mechanism to those of a small set of simpler problems easy to solve have been ideated for general-purpose software.

If the mechanism is a linkage (i.e. contains only lower pairs), structural decomposition [1] based on Assur groups (AGs) [2, 3] is the most known of these procedures. Such procedure decomposes the linkage into "drivers" whose motion is known and AGs whose kinematics is analytically solvable starting from position, velocity and acceleration of the connecting points. Other procedures [4] rely on systematic ways for writing and solving the constraint equations and their 1st and 2nd time derivatives. For planar linkages, such equations can be systematically written through the vector-loop method [4, 5, 6], which is easily implementable by using complex numbers[1] for representing planar vectors.

If the mechanism contains higher pairs (i.e., is not a linkage), its constraint equations, over the loop equations, must contain suitable auxiliary equations [11–16] that can be written in a systematic way. In this case, other approaches based on equivalent linkages [9, 17] or apparent velocity/acceleration equations [18] are more difficult to implement in general-purpose programs.

In the case of single-DOF planar mechanisms, the ratios between the secondary-variable[2] rates and the generalized-coordinate rate, named velocity (or influence) coefficients (VCs), together with their 1st derivative with respect to the generalized coordinate (acceleration coefficients (ACs)), have been proposed, first, for solving some issues of graphical techniques [19–21], then, for the systematic solution of kinematic analyses [11, 13, 22] and for dynamic analyses [23, 24], too. In addition, they have been used to identify the singular configurations (singularities) of these mechanisms [25]. The main feature of these coefficients is that they depend only on the mechanism configuration. Such property holds even though the single-DOF mechanism is not planar provided its constraints are scleronomic and holonomic, but it was not exploited for spatial mechanisms.

In the case of multi-DOF planar mechanisms (or scleronomic and holonomic spatial mechanisms), all the secondary variables depend only on the generalized coordinates, and their rates are linear combinations of generalized-coordinates' rates whose coefficients (influence coefficients (ICs)) depend only on the mechanism configuration [11]. Such ICs can be used for the mechanism kinematic analysis, but the resulting algorithm [11] sounds cumbersome and does not provide pieces of information on mechanism's singularities.

Here, with reference to multi-DOF planar mechanisms (or scleronomic and holonomic spatial mechanisms), first, the velocity-coefficient vector (VCV) and its Jacobian, named acceleration-coefficient Jacobian (ACJ), are introduced and proved to be the natural extension to multi-DOF mechanisms of VC and AC, respectively. Then, a general purpose algorithm based on the complex-number method and on the systematic use of VCVs and ACJs is presented for solving the kinematic analysis of any planar mechanism and for determining the extreme poses (dead center positions) of the links. Eventually, the proposed algorithm is applied to a case study for showing its effectiveness. As far as this author is aware, this is the first time that VCVs and ACJs are presented and

---

[1] The geometric interpretation of complex numbers [7, 8] is dated back to Wessel (1797), Argand (1806) and Gauss (1831). An exhaustive presentation of the analytic plane geometry through complex numbers is reported in [8]; whereas planar kinematics through complex numbers is fully presented in [9] and, in a less extensive way, in [10, 11].

[2] Hereafter, with reference to a multi-DOF mechanism, the phrase "generalized coordinates" will denote the input variables of the kinematic analysis; whereas, the phrase "secondary variable" will denote a geometric parameter that changes its value during the motion of the mechanism and is not a generalized coordinate.

exploited for determining the dead center positions of multi-DOF planar mechanisms. The proposed algorithm is efficient enough for constituting the kinematic block of any dynamic model of these mechanisms, and simple enough for being presented in graduate courses.

The paper is organized as follows. Section 2 introduces VCVs and ACJs and highlights their relationship with dead center positions. Section 3, first, recalls some background concepts on a general notation, previously presented by the author, which uses the complex-number method, then, presents the general purpose algorithm. Section 4 applies it to a relevant case study, and section 5 draws the conclusions.

2. Velocity-Coefficient Vectors (VCVs) and Acceleration-Coefficient Jacobians (ACJs)

The constraint equations of a multi-DOF holonomic scleronomous mechanism contain only the generalized coordinates, say ξ_j for j=1,…,f where f is the DOF number, and the secondary variables, say ζ_i for i=1,…,e, over the geometric constants of the links. Also, the number of constraint equations is equal to the number, e, of secondary variables that appear in them. Thus, the analytical (or numerical) solution of this constraint-equation system brings to write the i-th secondary variable, ζ_i, as a function of the generalized coordinates, that is, as follows

$$\zeta_i = \zeta_i(\xi_1, …, \xi_f) \qquad \text{i=1, …,e} \qquad (1)$$

The 1st time derivative of Eq. (1) yields

$$\dot{\zeta}_i = \mathbf{v}_i^T \dot{\boldsymbol{\xi}} \qquad \text{i=1, …,e} \qquad (2)$$

where $\boldsymbol{\xi}=(\xi_1, …, \xi_f)^T$ is the f-tuple collecting all the generalized coordinates, and $\mathbf{v}_i=(v_{i1}, …, v_{if})^T$ is an f-tuple whose entries depends only on the mechanism configuration (i.e., on $\boldsymbol{\xi}$). From an analytic point of view, the k-th entry, v_{ik}, of $\mathbf{v}_i$ is equal to the partial derivative $\dfrac{\partial \zeta_i}{\partial \xi_k}$ and the following relationship holds

$$\mathbf{v}_i = \nabla \zeta_i \qquad \text{i=1, …,e} \qquad (3)$$

where $\nabla(\cdot)$ denotes the gradient of the scalar function $(\cdot)$. Hereafter, $\mathbf{v}_i$ will be called *velocity-coefficient vector* (VCV) of the i-th secondary variable ζ_i.

The time derivative of Eq. (2) gives

$$\ddot{\zeta}_i = \mathbf{v}_i^T \ddot{\boldsymbol{\xi}} + \dot{\boldsymbol{\xi}}^T \boldsymbol{\Lambda}_i \dot{\boldsymbol{\xi}} \qquad \text{i=1, …,e} \qquad (4)$$

where $\boldsymbol{\Lambda}_i$ is the Jacobian of the velocity-coefficient vector $\mathbf{v}_i$, that is,

$$\boldsymbol{\Lambda}_i = \begin{bmatrix} \dfrac{\partial v_{i1}}{\partial \xi_1} & \cdots & \dfrac{\partial v_{i1}}{\partial \xi_f} \\ \vdots & \ddots & \vdots \\ \dfrac{\partial v_{if}}{\partial \xi_1} & \cdots & \dfrac{\partial v_{if}}{\partial \xi_f} \end{bmatrix} \qquad \text{i=1, …,e} \qquad (5)$$

The analytic meaning of $\mathbf{v}_i$ (i.e., Eq. (3)) brings to the conclusion that

$$\boldsymbol{\Lambda}_i = \mathbf{H}(\zeta_i) \qquad \text{i=1, …,e} \qquad (6)$$

where $\mathbf{H}(\cdot)$ denotes the Hessian matrix of the scalar function $(\cdot)$. Hereafter, $\boldsymbol{\Lambda}_i$ will be called *acceleration-coefficient Jacobian* (ACJ) of the i-th secondary variable ζ_i. Since ACJs are indeed Hessian of scalar-valued functions, they are always symmetric matrices with real entries.

2.1. Determination of Mechanism's Singularities

By considering mechanisms as input-output systems [26–28], mechanism's singular configurations (singularities) are those that make the instantaneous input-output relationship fails in stating a one-to-one

correspondence between input and output rates. Such configurations occur [25, 29] when an input (i.e., a generalized coordinate) and/or an output (i.e., a secondary variable) variable is at a stationary point[3] [29].

The system constituted by the e Eqs. (2) is a particular form of multi-DOF mechanism's instantaneous input-output relationship. According to Eqs. (2) and (3), the i-th secondary variable ζ_i is at a stationary point when

$$\mathbf{v}_i = \mathbf{0} \tag{7}$$

Vector Eq. (7) is a system of f non-linear equations in $\boldsymbol{\xi}$ whose solutions identify the mechanism singularities associated to the stationary points of ζ_i. Such points are extreme values of ζ_i (i.e., correspond to dead center positions) if all the eigenvalues of the Hessian matrix of ζ_i, evaluated at that point, have the same sign [30]. According to Eq. (6), this condition can be reformulated as follows: ζ_i reaches an extreme value in a configuration where its VCV, $\mathbf{v}_i$, is a null vector and its ACJ, $\boldsymbol{\Lambda}_i$, has eigenvalues[4] with the same sign.

Sometimes, the mechanism configurations that make a particular entry v_{ik} of $\mathbf{v}_i$ equal to zero may be relevant, too. They identify the extreme values ζ_i can reach by changing the k-th input variable while the other inputs are kept locked. From a kinematic point of view, the elementary variation of the k-th input variable has no effect on ζ_i when the mechanism is at one of these configurations.

The stationary points of the input variables can be determined by considering that, after a simple algebraic manipulation, Eqs. (2) yield

$$\dot{\xi}_j = \frac{1}{v_{ij}}\left(\dot{\zeta}_i - \sum_{\substack{k=1,f \\ k \neq j}} v_{ik}\dot{\xi}_k \right) \qquad \text{i=1, ...,e; j=1, ...,f} \tag{8}$$

Equation (8) brings to conclude that singularities related to stationary points of the j-th generalized coordinate, ξ_j, occur when any one of the coefficients $(1/v_{ij})$, for i=1,...,e, is equal to zero.

The highlighted singularity-identification capability make VCVs and ACJs the natural extension of single-DOF mechanisms' VCs and ACs[5] to multi-DOF mechanisms.

3. Kinematic Analysis of Multi-DOF Planar Mechanisms through VCVs and ACJs

Planar mechanisms contain only four types of kinematic pairs: two lower-pair types (i.e., revolute (R) or prismatic (P) pairs) and two higher-pair types (i.e., rolling (R_c) or sliding (S_c) contacts). The constraint equations of these kinematic pairs are all scleronomic and holonomic (i.e., contain only the generalized coordinates and can be put in the form of Eq. (1)) provided that the frame is at rest. Such equations can be systematically written as shown in [13] by using complex numbers both for the loop equations and for the auxiliary equations associated to the higher pairs. As a consequence, all results reported in the previous sections can be applied to multi-DOF planar mechanisms. In this section, first, the general notation, presented in [13], for systematically writing the constraint equations of planar mechanisms will be briefly recalled; then, a general algorithm, based on VCVs and ACJs, will be presented for solving velocity and acceleration analyses of multi-DOF planar mechanisms.

In planar multi-DOF mechanisms with f DOF, Gruebler's formula and Euler formula [11] yield[6]

$$c_1 = 1.5 \, m - 0.5 \, c_2 - 0.5 \, (f + 3) \tag{9a}$$
$$a = 0.5 \, m + 0.5 \, c_2 - 0.5 \, (f + 1) \tag{9b}$$

where m is the number of links, a is the number of independent loops, c_1 is the number of single-DOF kinematic pairs (i.e., whose type is R or P or R_c) and c_2 is the number of sliding contacts (S_c pairs), which are two-DOF kinematic pairs.

Mechanism's graph[7] allows the identification of the independent loops to use for writing the loop equations. Indeed, the circuits of this graph geometrically individuate closed polygonal chains (loops), embedded in the

---

[3] A stationary point of a differentiable multivariable function is any point at which its gradient is a null vector. Stationary points can be local extrema (that is, local minima or maxima) or saddle points. In planar mechanisms, local extrema of an input (output) variable corresponds to dead center positions (i.e., mechanism singularities) of the input (output) link the variable refers to.

[4] Eigenvalues of real symmetric matrices are all real.

[5] It is worth reminding that, in single-DOF mechanisms, the zeroing of a VC identifies a singularity [25].

[6] Equation (9a) is the Gruebler's formula for planar mechanisms [i.e., f=3(m−1)−2c_1−c_2] written by isolating c_1; whereas, Eq. (9b) is obtained from the Euler formula for planar mechanisms (i.e., a=c_1+c_2−m+1), which comes from graph theory [11], by replacing c_1 with its explicit expression (9a).

[7] The graph of a mechanism fully represents its topology by stating a one-to-one correspondence between nodes (edges) and links (kinematic pairs) [11].

linkage. In these loops, the vertices are either points of R-pair axes, or contact points of higher pairs (i.e., R_c or S_c pairs), or points of P-pair sliding directions, which are fixed to one or the other of the two links joined by the P pair; whereas, the edges are either constant-length segments fixed to one link or variable-length segments corresponding to the joint variables of the P pairs or variable-lengths distances of higher-pairs' contact points from points fixed to either of the two links joined by those contacts [13].

The loop equations can be systematically written by implementing the following steps:

i) the links are numbered from 1 to m and the number, a, of independent loops is computed from Eq. (9b);

ii) by inspecting all the kinematic pairs, c_1+c_2 points, A_t for $t = 1,…, c_1+c_2$, (one for each pair), which are the contact points of the higher pairs plus points that belong either to an R-pair axis or to a line parallel to a P-pair sliding direction, are selected;

iii) among the points A_t for $t = 1,…, c_1+c_2$, the couples of points that can be joined through an oriented segment either embedded in a link or belonging to a line parallel to a P-pair sliding direction are joined;

iv) the net of oriented segments deduced in step (iii) is analyzed and, through the graph of the mechanism, the independent loops are chosen; then, a complex number is associated to each oriented segment belonging to the chosen loops, and, by assigning a conventional positive direction (clockwise or counterclockwise) to each loop, the following loop equations are written:

$$\sum_{k \in L_j} \pm \mathbf{z}_{kj} = 0 \qquad\qquad j = 1, …, a \qquad (10)$$

where L_j is a set collecting the integer numbers that identify the links traversed by the j-th loop, $\mathbf{z}_{kj}$ is the complex number associated to the k-th edge of the j-th loop, and the sign + or − depends on whether the direction of the oriented segment represented by $\mathbf{z}_{kj}$ concurs or not with the positive direction (clockwise or counterclockwise) assigned to the j-th loop.
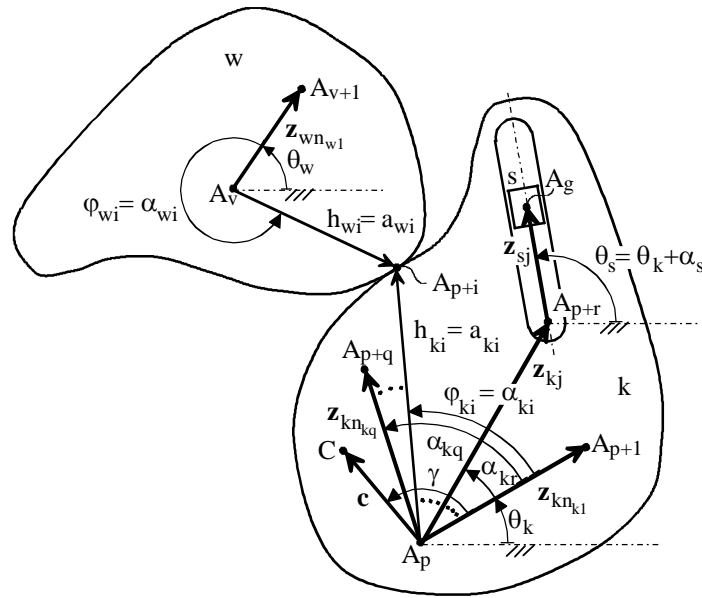

Figure 1: Notations introduced in [13]: k-th link, traversed by q independent loops, in contact with the w-th link at A_{p+i} through an higher pair, and containing the linear guide of a P-pair that connects it to a slider fixed in the s-th link.

The general expressions of the complex numbers, $\mathbf{z}_{kj}$, appearing in Eq. (10) can be written by using the general notation introduced in [13]. Figure 1 is extracted from [13], and shows this notation with reference to a generic k-th link traversed by q independent loops. Such k-th link contains the linear guide of a P-pair that connects it to a slider fixed in the s-th link, and the contact point, A_{p+i} of an higher pair that connects it to the w-th link [h_{ki} (h_{wi}) and φ_{ki} (φ_{wi}) are the polar coordinates that define the conjugate profile fixed to the k-th link (to the w-th link) as a function of the curve parameter ψ_{ki} (the curve parameter ψ_{wi})]. With reference to Fig. 1, the possible $\mathbf{z}_{kj}$ that can be defined are

$$\mathbf{z}_{kj} = \mathbf{a}_{kj}\, \mathbf{u}_k \qquad\qquad j \in N_k = \{n_{k1},…,n_{kq}\} \subseteq \{1, …, a\} \qquad (11a)$$
$$\mathbf{z}_{sj} = d_s\, \mathbf{u}_s \qquad\qquad\qquad (11b)$$

5

where, N_k is the subset of $\{1, \ldots, a\}$ that collects the integer numbers identifying the loops passing through the k-th link. s is the number identifying the link that, in the j-th loop, follows[8] the k-th link. d_s is the variable length of the segment $A_{(p+r)}A_g$ (i.e., it is the joint variable of the P pair),

$$\mathbf{a}_{kj} = a_{kr}\exp(\mathbf{i}\alpha_{kr}) \qquad \mathbf{u}_k = \exp(\mathbf{i}\theta_k), \qquad \mathbf{u}_s = \exp(\mathbf{i}\alpha_s)\,\mathbf{u}_k, \tag{16}$$

where $\mathbf{i}$ is the imaginary unit $\sqrt{-1}$. If $j=n_{ki}$ (i.e., if r=i) $a_{kr}=h_{ki}(\psi_{ki})$ and $\alpha_{kr}= \varphi_{ki}(\psi_{ki})$, otherwise (i.e., $j\neq n_{ki}$ and $r\neq i$), a_{kr} is the constant length of segment $A_pA_{(p+r)}$, whereas, α_{kr}, for r $\in\{2, \ldots, i-1, i+1, \ldots, q\}$, together with α_s, are constant angles. θ_k, for $k = 1,\ldots, m$, is the angle that defines the orientation of the k-th link with respect to the frame.

The above-recalled notation was presented in [13]. It has the particular feature of introducing only one variable for each mobile link, which is an angle, θ_k, or a linear variable, d_s, if the link is connected to the previous one through an R-pair or a P-pair, respectively, and two curve parameters, ψ_{ki} and ψ_{wi}, for each R_c-pair or S_c-pair. The above-introduced loop-equation system (Eqs. (10)) is a system of 2a $[=(m-1)+c_2-f$ (see Eq. (9b))] scalar equations, which contains $(m-1)+2(c_2+c_{Rc})$ variables where c_{Rc} is the number of R_c pairs. Thus, c_2+2c_{Rc} auxiliary constraint equations, due to the higher pairs, must be added to obtain a constraint-equation system solvable once the f generalized coordinates are assigned. Such auxiliary equations (see [13] for details) can be put in the following form[9]

$$\mathbf{z}_{Rc|i}(\psi_{i1}, \psi_{i2}, \theta_{i1}, \theta_{i2}) = 0 \qquad\qquad i = 1, \ldots, c_{Rc} \quad (17a)$$
$$\mathbf{z}_{Sc|n}(\psi_{n1}, \psi_{n2}, \theta_{n1}, \theta_{n2}) = 0 \qquad\qquad n = 1, \ldots, c_2 \quad (17b)$$

where $\mathrm{Im}(\mathbf{z}_{Sc|n})$ is always equal to zero. Equations (17) do not add further variables.

Equations (10) and (17) constitute the constraint-equation system of the mechanism. Such system contains $e=2a+c_2+2c_{Rc}$ $[=(m-1)+ 2(c_2+c_{Rc})-f]$ secondary variables and as many scalar equations. Once the f generalized coordinates are assigned, all the secondary variables can be computed by solving (either, when possible, analytically or, always, numerically) this system. Such computation is the position analysis (PA) of the mechanism and is the first step of the kinematic analysis. Once the PA has been solved all the complex numbers appearing in the constraint equations are known and can be included in the input data of the velocity (VA) and acceleration (AA) analyses.

The 1st and 2nd time derivatives of the complex numbers appearing in Eqs. (10) and (17) can be formally written as follows:

$$\dot{\mathbf{z}}_{kj} = \dot{\boldsymbol{\xi}}^T\,(\mathbf{a}_{kj}'\boldsymbol{\varepsilon}_{kr} + \mathbf{a}_{kj}\mathbf{v}_k\mathbf{i})\,\mathbf{u}_k\,; \qquad \dot{\mathbf{z}}_{sj} = \dot{\boldsymbol{\xi}}^T\,(\boldsymbol{\delta}_s + d_s\mathbf{v}_k\mathbf{i})\,\mathbf{u}_s\,; \tag{18a}$$

$$\ddot{\mathbf{z}}_{kj} = \ddot{\boldsymbol{\xi}}^T\,(\mathbf{a}_{kj}'\boldsymbol{\varepsilon}_{kr} + \mathbf{a}_{kj}\mathbf{v}_k\mathbf{i})\,\mathbf{u}_k + \dot{\boldsymbol{\xi}}^T\,\{(\mathbf{a}_{kj}'\boldsymbol{\Gamma}_{kr} + \mathbf{a}_{kj}\boldsymbol{\Lambda}_k\mathbf{i})\,\mathbf{u}_k + [(\mathbf{a}_{kj}''\boldsymbol{\varepsilon}_{kr} + \mathbf{a}_{kj}'\mathbf{v}_k\mathbf{i})\mathbf{u}_k\boldsymbol{\varepsilon}_{kr}^T] + (\mathbf{a}_{kj}'\boldsymbol{\varepsilon}_{kr}\mathbf{i} - \mathbf{a}_{kj}\mathbf{v}_k)\mathbf{u}_k\mathbf{v}_k^T\}\,\dot{\boldsymbol{\xi}}\,; \tag{18b}$$

$$\ddot{\mathbf{z}}_{sj} = \ddot{\boldsymbol{\xi}}^T\,(\boldsymbol{\delta}_s + d_s\mathbf{v}_k\mathbf{i})\,\mathbf{u}_s + \dot{\boldsymbol{\xi}}^T\,\{[\boldsymbol{\Lambda}_s + d_s(\boldsymbol{\Lambda}_k\mathbf{i} - \mathbf{v}_k\mathbf{v}_k^T) + \mathbf{i}(\boldsymbol{\delta}_s\mathbf{v}_k^T + \mathbf{v}_k\boldsymbol{\delta}_s^T)]\mathbf{u}_s\}\,\dot{\boldsymbol{\xi}}\,; \tag{18c}$$

$$\dot{\mathbf{z}}_{Rc|i} = \dot{\boldsymbol{\xi}}^T\,\mathbf{L}_{Rc|i} \quad, \qquad \ddot{\mathbf{z}}_{Rc|i} = \ddot{\boldsymbol{\xi}}^T\,\mathbf{L}_{Rc|i} + \dot{\boldsymbol{\xi}}^T\,\big(\mathbf{M}_{Rc|i} + \mathbf{G}_{Rc|i}\big)\dot{\boldsymbol{\xi}} \tag{18c}$$

$$\dot{\mathbf{z}}_{Sc|n} = \dot{\boldsymbol{\xi}}^T\,\mathbf{L}_{Sc|n}, \qquad \ddot{\mathbf{z}}_{Sc|n} = \ddot{\boldsymbol{\xi}}^T\,\mathbf{L}_{Sc|n} + \dot{\boldsymbol{\xi}}^T\,\big(\mathbf{M}_{Sc|n} + \mathbf{G}_{Sc|n}\big)\dot{\boldsymbol{\xi}} \tag{18d}$$

where[10]

$$\mathbf{L}_{Rc|i} = \frac{\partial\mathbf{z}_{Rc|i}}{\partial\psi_{i1}}\boldsymbol{\varepsilon}_{i1} + \frac{\partial\mathbf{z}_{Rc|i}}{\partial\psi_{i2}}\boldsymbol{\varepsilon}_{i2} + \frac{\partial\mathbf{z}_{Rc|i}}{\partial\theta_{i1}}\mathbf{v}_{i1} + \frac{\partial\mathbf{z}_{Rc|i}}{\partial\theta_{i2}}\mathbf{v}_{i2}\,, \qquad \mathbf{M}_{Rc|i} = \frac{\partial\mathbf{z}_{Rc|i}}{\partial\psi_{i1}}\boldsymbol{\Gamma}_{i1} + \frac{\partial\mathbf{z}_{Rc|i}}{\partial\psi_{i2}}\boldsymbol{\Gamma}_{i2} + \frac{\partial\mathbf{z}_{Rc|i}}{\partial\theta_{i1}}\boldsymbol{\Lambda}_{i1} + \frac{\partial\mathbf{z}_{Rc|i}}{\partial\theta_{i2}}\boldsymbol{\Lambda}_{i2} \quad (19a)$$

$$\mathbf{L}_{Sc|n} = \frac{\partial\mathbf{z}_{Sc|n}}{\partial\psi_{n1}}\boldsymbol{\varepsilon}_{n1} + \frac{\partial\mathbf{z}_{Sc|n}}{\partial\psi_{n2}}\boldsymbol{\varepsilon}_{n2} + \frac{\partial\mathbf{z}_{Sc|n}}{\partial\theta_{n1}}\mathbf{v}_{n1} + \frac{\partial\mathbf{z}_{Sc|n}}{\partial\theta_{n2}}\mathbf{v}_{n2}\,, \qquad \mathbf{M}_{Sc|n} = \frac{\partial\mathbf{z}_{Sc|n}}{\partial\psi_{n1}}\boldsymbol{\Gamma}_{n1} + \frac{\partial\mathbf{z}_{Sc|i}}{\partial\psi_{n2}}\boldsymbol{\Gamma}_{n2} + \frac{\partial\mathbf{z}_{Sc|n}}{\partial\theta_{n1}}\boldsymbol{\Lambda}_{n1} + \frac{\partial\mathbf{z}_{Sc|i}}{\partial\theta_{n2}}\boldsymbol{\Lambda}_{n2} \quad (19b)$$

---

[8] In the j-th loop, the link order that states which is the previous or the next link is given by the positive direction (clockwise or counterclockwise) assigned to the j-th loop. Also, the order of the loops is given by the index j of system (10). Accordingly, the variables are defined.

[9] In Eqs. (17), ψ_{i1}, and ψ_{i2} (ψ_{n1}, and ψ_{n2}) are the curve parameters of the two conjugate profiles in contact at the i-th R_c-pair (the n-th S_c-pair); whereas, θ_{i1}, and θ_{i2} (θ_{n1}, and θ_{n2}) are the angular variables associated to the two links in contact at the i-th R_c-pair (the n-th S_c-pair). The analytic expressions of the complex numbers $\mathbf{z}_{Rc|i}$ and $\mathbf{z}_{Sc|n}$ are reported in [13].

[10] Formulas (19c) are compact expressions where the partial derivatives of the f-tuple $\mathbf{L}_{Rc|i}$ ($\mathbf{L}_{Sc|i}$) must be done by considering the entries of the VCVs as if they were independent variables.

$$\mathbf{G}_{\text{Rc}|i} = \frac{\partial \mathbf{L}_{\text{Rc}|i}}{\partial \psi_{i1}} \boldsymbol{\varepsilon}_{i1}^{\text{T}} + \frac{\partial \mathbf{L}_{\text{Rc}|i}}{\partial \psi_{i2}} \boldsymbol{\varepsilon}_{i2}^{\text{T}} + \frac{\partial \mathbf{L}_{\text{Rc}|i}}{\partial \theta_{i1}} \mathbf{v}_{i1}^{\text{T}} + \frac{\partial \mathbf{L}_{\text{Rc}|i}}{\partial \theta_{i2}} \mathbf{v}_{i2}^{\text{T}}, \qquad \mathbf{G}_{\text{Sc}|n} = \frac{\partial \mathbf{L}_{\text{Sc}|n}}{\partial \psi_{n1}} \boldsymbol{\varepsilon}_{n1}^{\text{T}} + \frac{\partial \mathbf{L}_{\text{Sc}|n}}{\partial \psi_{n2}} \boldsymbol{\varepsilon}_{n2}^{\text{T}} + \frac{\partial \mathbf{L}_{\text{Sc}|n}}{\partial \theta_{n1}} \mathbf{v}_{n1}^{\text{T}} + \frac{\partial \mathbf{L}_{\text{Sc}|n}}{\partial \theta_{n2}} \mathbf{v}_{n2}^{\text{T}} \quad (19c)$$

The matrix $\mathbf{M}_{\text{Rc}|i}$ ($\mathbf{M}_{\text{Sc}|n}$) is a linear combination of ACJs, which are symmetric matrices; thus, it is a symmetric matrix. Also, it is easy to demonstrate (see the Appendix) that the matrix $\mathbf{G}_{\text{Rc}|i}$ ($\mathbf{G}_{\text{Sc}|n}$) is symmetric, too.

In Eqs. (18) and (19), the following VCVs and ACJs have been introduced

$$\mathbf{v}_k = \nabla \theta_k, \qquad \boldsymbol{\delta}_s = \nabla d_s, \qquad \boldsymbol{\varepsilon}_{kr} = \nabla \psi_{kr}, \qquad\qquad (20a)$$

$$\boldsymbol{\Lambda}_k = \begin{bmatrix} \dfrac{\partial v_{k1}}{\partial \xi_1} & \cdots & \dfrac{\partial v_{k1}}{\partial \xi_f} \\ \vdots & \ddots & \vdots \\ \dfrac{\partial v_{kf}}{\partial \xi_1} & \cdots & \dfrac{\partial v_{kf}}{\partial \xi_1} \end{bmatrix} = \mathbf{H}(\theta_k), \quad \boldsymbol{\Delta}_s = \begin{bmatrix} \dfrac{\partial \delta_{s1}}{\partial \xi_1} & \cdots & \dfrac{\partial \delta_{s1}}{\partial \xi_f} \\ \vdots & \ddots & \vdots \\ \dfrac{\partial \delta_{sf}}{\partial \xi_1} & \cdots & \dfrac{\partial \delta_{sf}}{\partial \xi_f} \end{bmatrix} = \mathbf{H}(d_s), \quad \boldsymbol{\Gamma}_{kr} = \begin{bmatrix} \dfrac{\partial \varepsilon_{kr1}}{\partial \xi_1} & \cdots & \dfrac{\partial \varepsilon_{kr1}}{\partial \xi_f} \\ \vdots & \ddots & \vdots \\ \dfrac{\partial \varepsilon_{krf}}{\partial \xi_1} & \cdots & \dfrac{\partial \varepsilon_{krf}}{\partial \xi_f} \end{bmatrix} = \mathbf{H}(\psi_{kr})$$

$$(20b)$$

together with the conjugate profile's geometric data $\mathbf{a}'_{kj}$ and $\mathbf{a}''_{kj}$ defined as follows

$$\mathbf{a}'_{kj} = \frac{d\mathbf{a}_{kj}}{d\psi_{kr}}, \qquad \mathbf{a}''_{kj} = \frac{d^2\mathbf{a}_{kj}}{d\psi_{kr}^2} = \frac{d\mathbf{a}'_{kj}}{d\psi_{kr}} \qquad\qquad (21)$$

where, if $\mathbf{z}_{kj}$ refers to a free vector pointing to an higher-pair contact point, ψ_{kr} is the curve parameter of the conjugate profile of that higher pair, which is fixed to the k-th link, and $\boldsymbol{\varepsilon}_{kr}$ ($\boldsymbol{\Gamma}_{kr}$) is really a VCV (an ACJ); otherwise, $\boldsymbol{\varepsilon}_{kr} = \mathbf{0}, \boldsymbol{\Gamma}_{kr} = \mathbf{0}, \mathbf{a}'_{kj} = \mathbf{a}''_{kj} = 0$, and formulas (18a) and (18b) become

$$\dot{\mathbf{z}}_{kj|0} = \dot{\boldsymbol{\xi}}^{\text{T}} \mathbf{v}_k \mathbf{i} \mathbf{z}_{kj}; \qquad \ddot{\mathbf{z}}_{kj|0} = \ddot{\boldsymbol{\xi}}^{\text{T}} \mathbf{v}_k \mathbf{i} \mathbf{z}_{kj} + \dot{\boldsymbol{\xi}}^{\text{T}} [(\boldsymbol{\Lambda}_k \mathbf{i} - \mathbf{v}_k \mathbf{v}_k^{\text{T}}) \mathbf{z}_{kj}] \dot{\boldsymbol{\xi}}; \qquad\qquad (22)$$

It is worth noting that, in formulas (19), VCVs' and ACJs' coefficients are all known functions of the mechanism configuration, which can be analytically determined through the general explicit expressions of $\mathbf{z}_{\text{Rc}|i}$ and $\mathbf{z}_{\text{Sc}|n}$ reported in [13].

The kinematic interpretation of formulas (18) is (see Fig. 1)

$$\dot{\mathbf{z}}_{kj} - \dot{\boldsymbol{\xi}}^{\text{T}} \boldsymbol{\varepsilon}_{kr} \mathbf{a}'_{kj} \mathbf{u}_k = \dot{\boldsymbol{\xi}}^{\text{T}} \mathbf{v}_k \mathbf{i} \mathbf{z}_{kj} = \mathbf{v}_{A_{(p+r)}|k} - \mathbf{v}_{A_p|k}; \qquad\qquad (23a)$$

$$\ddot{\mathbf{z}}_{kj} - \ddot{\boldsymbol{\xi}}^{\text{T}} \mathbf{a}'_{kj} \boldsymbol{\varepsilon}_{kr} - \dot{\boldsymbol{\xi}}^{\text{T}} \{[\mathbf{a}'_{kj} \boldsymbol{\Gamma}_{kr} + \mathbf{a}''_{kj} \boldsymbol{\varepsilon}_{kr} \boldsymbol{\varepsilon}_{kr}^{\text{T}} + \mathbf{a}'_{kj} \mathbf{i} (\mathbf{v}_k \boldsymbol{\varepsilon}_{kr}^{\text{T}} + \boldsymbol{\varepsilon}_{kr} \mathbf{v}_k^{\text{T}})] \mathbf{u}_k\} \dot{\boldsymbol{\xi}} = \ddot{\boldsymbol{\xi}}^{\text{T}} \mathbf{v}_k \mathbf{i} \mathbf{z}_{kj} + \dot{\boldsymbol{\xi}}^{\text{T}} \{(\boldsymbol{\Lambda}_k \mathbf{i} - \mathbf{v}_k \mathbf{v}_k^{\text{T}}) \mathbf{z}_{kj}\} \dot{\boldsymbol{\xi}} = \mathbf{a}_{A_{(p+r)}|k} - \mathbf{a}_{A_p|k}$$

$$(23b)$$

$$\dot{\mathbf{z}}_{sj} = \mathbf{v}_{Ag|s} - \mathbf{v}_{A_{(p+r)}|k}; \qquad\qquad (23c)$$

$$\ddot{\mathbf{z}}_{sj} = \mathbf{a}_{Ag|s} - \mathbf{a}_{A_{(p+r)}|k}; \qquad\qquad (23d)$$

where the symbol $\mathbf{v}_{B|g}$ ($\mathbf{a}_{B|g}$) denotes the velocity (acceleration), with respect to the frame, of a point B fixed to the g-th link, when expressed by using complex numbers. Moreover, with reference to the introduced notations and the loop n_{ki} of Fig. 1 (i.e., the path $A_pA_{(p+i)}A_v$), the following relationships hold ($j = n_{ki}$):

$$\dot{\mathbf{z}}_{kn_{ki}} - \dot{\mathbf{z}}_{wn_{ki}} = \mathbf{v}_{A_v|w} - \mathbf{v}_{A_p|k}; \qquad\qquad (24a)$$

$$\ddot{\mathbf{z}}_{kn_{ki}} - \ddot{\mathbf{z}}_{wn_{ki}} = \mathbf{a}_{A_v|w} - \mathbf{a}_{A_p|k}; \qquad\qquad (24b)$$

Once the PA has been solved, only the entries of VCVs and ACJs are unknown in the above-reported explicit expressions (18) and (19).

3.1. Velocity Analysis

Once the PA has been solved all the complex numbers appearing in the constraint-equation system (i.e., Eqs. (10) and (17)) are known, and, together with generalized-coordinates' rates, $\dot{\boldsymbol{\xi}}$, become the input data of the velocity analysis (VA). The 1st time derivative of Eqs. (10) and (17) provides the VA equations to solve. The VA equations can be automatically obtained by replacing, in the constraint-equation system, each complex

number with the expression of its 1ˢᵗ time derivative, formulas (18) provide. In so doing, the following system of VA equations is obtained

$$\dot{\xi}^T \mathbf{D}_j(\xi) = 0 \qquad\qquad j = 1, ..., a \qquad (25a)$$

$$\dot{\xi}^T \mathbf{L}_{Rc|i}(\xi) = 0 \qquad\qquad i = 1, ..., c_{Rc} \qquad (25b)$$

$$\dot{\xi}^T \mathbf{L}_{Sc|n}(\xi) = 0 \qquad\qquad n = 1, ..., c_2 \qquad (25c)$$

with $\mathbf{L}_{Rc|i}$ ($\mathbf{L}_{Sc|n}$) given by Eq. (19a) (Eq. (19b)), and

$$\mathbf{D}_j(\xi) = \sum_{k \in L_j} \pm [\mathbf{a}_{kj} \varepsilon_{kr} \mathbf{u}_k + \mathbf{v}_k \mathbf{i}(\mathbf{z}_{kj} + \beta_{kj} d_s \mathbf{u}_s) + \beta_{kj} \delta_s \mathbf{u}_s] \qquad (26)$$

where β_{kj} is equal to 1 if, in the j-th independent loop, the k-th link is connected to the next through a P pair, otherwise it is equal to 0. Of course, the VCV, say $\mathbf{v}_p$, that corresponds to the p-th variable chosen as generalized coordinates is a constant unit f-tuples whose entries, $v_{pk} = \dfrac{\partial \dot{\xi}_p}{\partial \dot{\xi}_k}$ for k=1,...,f, are equal to the Kronecker delta δ_{pk}. Also, the VCV that corresponds to the frame is a null vector. As a consequence, the ACJs corresponding to all the generalized coordinates and to the frame are always null matrices.

$\mathbf{D}_j$, $\mathbf{L}_{Rc|i}$, and $\mathbf{L}_{Sc|n}$ are f-dimensional vectors (f-tuples). Their above-reported explicit expressions are linear combinations of VCVs (which are all f-tuples with real entries) whose coefficients are complex numbers that are all known functions of ξ after the PA solution. In short, they are f-tuples with complex entries. Since Eqs. (25a), (25b), and (25c) must hold for any value set of the generalized-coordinates' rates, $\dot{\xi}$, system (25) is satisfied if and only if these f-tuples are null vectors, that is

$$\mathbf{D}_j = \mathbf{0} \qquad\qquad j = 1, ..., a \qquad (27a)$$

$$\mathbf{L}_{Rc|i} = \mathbf{0} \qquad\qquad i = 1, ..., c_{Rc} \qquad (27b)$$

$$\mathbf{L}_{Sc|n} = \mathbf{0} \qquad\qquad n = 1, ..., c_2 \qquad (27c)$$

System (27) is a linear system of $f(2(a+c_{Rc})+c_2)$ [$=f((m-1)+ 2(c_2+c_{Rc})-f)$] scalar equations in as many unknowns, which are the f real entries of the e [$=2(a+c_{Rc})+c_2$] VCVs of the secondary variables. The solution of system (27) is straightforward.

All the VCVs are known after the solution of system (27), and the velocity of any point of the mechanism can be computed by exploiting formulas (18a), (18b), (18c), together with their kinematic interpretation (23) and (24) as follows (see Fig. 1):

$$\mathbf{v}_{C|k} = \mathbf{v}_{A_p|k} + \mathbf{i}\,\dot{\xi}^T \mathbf{v}_k \, \mathbf{c} \qquad (28)$$

where $\mathbf{v}_{A_p|k}$ is computed by using one of the paths that joins point A_p to the frame through the edges of the independent loops and formulas (18), (23) and (24) (i.e., it is a particular algebraic sum of the terms, given by formulas (18), associated to the edges of this path); whereas, $\mathbf{c} = c \exp(i\gamma) \mathbf{u}_k$ with c equal to the constant length of the segment CA_p (see Fig.1).

Once the VA has been solved all the computed VCVs together with the results of the PA, $\dot{\xi}$, and $\ddot{\xi}$ become the input data of the acceleration analysis (AA).

3.2. Acceleration Analysis
The 2ⁿᵈ time derivative of Eqs. (10) and (17) provides the AA equations to solve. Such AA equations can be automatically obtained by replacing, in Eqs. (10) and (17), each complex number with the expression of its 2ⁿᵈ time derivative, formulas (18) provide. In so doing, the following system of AA equations is obtained

$$\ddot{\xi}^T \mathbf{D}_j(\xi) + \dot{\xi}^T [\mathbf{E}_j(\xi) - \mathbf{F}_j(\xi)]\dot{\xi} = 0 \qquad\qquad j = 1, ..., a \qquad (29a)$$

$$\ddot{\xi}^T \mathbf{L}_{Rc|i} + \dot{\xi}^T \left(\mathbf{M}_{Rc|i} + \mathbf{G}_{Rc|i}\right)\dot{\xi} = 0 \qquad\qquad i = 1, ..., c_{Rc} \qquad (29b)$$

$$\ddot{\xi}^T \mathbf{L}_{Sc|n} + \dot{\xi}^T \left(\mathbf{M}_{Sc|n} + \mathbf{G}_{Sc|n}\right)\dot{\xi} = 0 \qquad\qquad n = 1, ..., c_2 \qquad (29c)$$

with

$$\mathbf{E}_j(\xi) = \sum_{k \in L_j} \pm [\mathbf{a}_{kj} \Gamma_{kr} \mathbf{u}_k + \Lambda_k \mathbf{i}(\mathbf{z}_{kj} + \beta_{kj} d_s \mathbf{u}_s) + \beta_{kj} \Lambda_s \mathbf{u}_s] \qquad (30a)$$

8

$$\mathbf{F}_j(\xi) = \sum_{k \in L_j} \pm \{\mathbf{v}_k \mathbf{v}_k^T \mathbf{z}_{kj} - [\mathbf{a}_{kj}'' \boldsymbol{\varepsilon}_{kr} \boldsymbol{\varepsilon}_{kr}^T + \mathbf{a}_{kj}' \mathbf{i}(\mathbf{v}_k \boldsymbol{\varepsilon}_{kr}^T + \boldsymbol{\varepsilon}_{kr} \mathbf{v}_k^T)]\mathbf{u}_k - \beta_{kj}[\mathbf{i}(\boldsymbol{\delta}_s \mathbf{v}_k^T + \mathbf{v}_k \boldsymbol{\delta}_s^T) - d_s \mathbf{v}_k \mathbf{v}_k^T]\mathbf{u}_s\} \qquad (30b)$$

The analysis of Eqs. (30) reveals that the f×f matrices $\mathbf{E}_j$ and $\mathbf{F}_j$ are both linear combinations of symmetric matrices; thus, they are symmetric matrices, too. Since $\mathbf{D}_j$, $\mathbf{L}_{Rc|i}$ and $\mathbf{L}_{Sc|n}$ are all null f-tuples (see system (27)), system (29) is satisfied by imposing that the three quadratic terms appearing in it are all equal to zero for any value set of $\dot{\xi}$. Since these three quadratic terms involve always symmetric matrices, such condition is satisfied if and only if these symmetric matrices are null matrices, that is,

$$\mathbf{E}_j = \mathbf{F}_j \qquad\qquad j = 1, \ldots, a \qquad (31a)$$
$$\mathbf{M}_{Rc|i} = -\mathbf{G}_{Rc|i} \qquad\qquad i = 1, \ldots, c_{Rc} \qquad (31b)$$
$$\mathbf{M}_{Sc|n} = -\mathbf{G}_{Sc|n} \qquad\qquad n = 1, \ldots, c_2 \qquad (31c)$$

System (31) is a linear system whose unknowns are the entries of the ACJs. In system (31), $\mathbf{F}_j$, $\mathbf{G}_{Rc|i}$ and $\mathbf{G}_{Sc|n}$ are all known matrices since they contain only VCVs and complex numbers, which are known after the PA solution; whereas, $\mathbf{E}_j$, $\mathbf{M}_{Rc|i}$ and $\mathbf{M}_{Sc|n}$ are all linear combinations of the ACJs whose coefficients are the same that multiply the corresponding VCVs in the explicit expression of $\mathbf{D}_j$, $\mathbf{L}_{Rc|i}$ and $\mathbf{L}_{Sc|n}$ (see Eqs. (19a), (19b) and (26)), respectively. Also, all the matrices are symmetric. Therefore, system (31) is constituted by $2(a+c_{Rc})+c_2$ [= $(m-1)+ 2(c_2+c_{Rc})-f$] f×f-symmetric-matrix equations that correspond to $f(f+1)(2(a+c_{Rc})+c_2)/2$ scalar equations in as many unknowns, which are the entries of the e [=$2(a+c_{Rc})+c_2$] ACJs[11]. The solution of system (31) is straightforward.

All the ACJs are known after the solution of system (31). Thus, the acceleration of any point of the mechanism can be computed by exploiting formulas (18a), (18b), (18c), and their kinematic interpretation (23) and (24) as follows (see Fig. 1)

$$\mathbf{a}_{C|k} = \mathbf{a}_{A_p|k} + [\ddot{\xi}^T \mathbf{v}_k \mathbf{i} + \dot{\xi}^T (\boldsymbol{\Lambda}_k \mathbf{i} - \mathbf{v}_k \mathbf{v}_k^T) \dot{\xi}]\mathbf{c} \qquad (32)$$

where $\mathbf{a}_{A_p|k}$ is computed by using one of the paths that joins point A_p to the frame through the edges of the independent loops and formulas (18), (23) and (24) (i.e., it is a particular algebraic sum of the terms, given by formulas (18), associated to the edges of this path).

3.3. Singularity Analysis
If the VCVs and ACJs have been computed as a function of the mechanism configuration (i.e., of ξ), the singular configurations (singularities) of the mechanisms can be identified by exploiting their properties (see subsection 2.1). In particular, the following steps can be implemented:

- for each secondary variable, ζ_i for i=1,…,e,
   i)   the values of ξ that make the corresponding VCV, say $\mathbf{v}_i$, a null vector (i.e., that satisfy Eq.(7)) are computed;
   ii) for each ξ value computed at the previous step, the entries of the corresponding ACJ, say $\boldsymbol{\Lambda}_i$, are computed and the eigenvalues of the so-computed $\boldsymbol{\Lambda}_i$ are determined;
   iii) if all the computed eigenvalues have the same sign, the ξ value identifies a mechanism configuration at which the secondary variable ζ_i reaches an extreme value (i.e., a dead center position); otherwise, it identifies a saddle point of ζ_i.
- for each generalized coordinate, ξ_j for j=1,…,f,
   I)   the corresponding f Eqs. (8) are considered, and the ξ values that make at least one of the coefficients $(1/\nu_{ij})$, for i=1,…,e, equal to zero are determined;
   II) the ξ_j components of the ξ values determined at the previous step are compared to identify the extreme values and the corresponding mechanism configurations.

It is worth noting that the extreme values of the secondary variables could be determined by direct comparison, as same as the ones of the generalized coordinates, without using the ACJs.

---

[11] Due to the ACJ symmetry, there are $f(f+1)/2$ independent entries for each ACJ.

4. Case Study

In this section, the use and the effectiveness of the above-proposed kinematic-analysis algorithm are illustrated by applying it to the five-bar linkage (Fig. 2), which is commonly used as a benchmark for testing algorithms conceived for planar multi-DOF mechanisms.

The five-bar linkage (Fig. 2) has $m=5$, $c_1=5$ and $c_2=0$; hence, Eqs. (9) yield $f=2$ and $a=1$. Accordingly, the inspection of the five R-pairs brings to individuate the five points A_r, $r=1,\ldots,5$, shown in Fig. 2, as the vertices of the only loop embedded in the mechanism: loop $A_1A_2A_3A_4A_5A_1$.

4.1. Position Analysis

Since the studied mechanism is a linkage its constraint equations coincide with its loop equations. The loop equation of the above-identified unique loop is (the complex number are referred to the Argand plane A_1xy fixed to the frame (Fig. 2))

$$\mathbf{z}_{21} + \mathbf{z}_{31} - \mathbf{z}_{11} - \mathbf{z}_{41} - \mathbf{z}_{51} = \mathbf{0} \tag{33}$$

where [$\mathbf{u}_1 = 1$; $\mathbf{u}_k = \exp(i\theta_k)$ for $k= 2,\ldots,5$; the chosen generalized coordinates are $\xi_1=\theta_2$ and $\xi_2=\theta_5$]

$$\mathbf{z}_{11} = a_{11}; \quad \mathbf{z}_{21} = a_{21}\,\mathbf{u}_2; \quad \mathbf{z}_{31} = a_{31}\,\mathbf{u}_3; \quad \mathbf{z}_{41} = a_{41}\,\mathbf{u}_4; \quad \mathbf{z}_{51} = a_{51}\,\mathbf{u}_5; \tag{34}$$

The two secondary variables, θ_3 and θ_4, can be expressed as a function of the generalized coordinates by isolating $\mathbf{z}_{31}$ ($\mathbf{z}_{41}$) in Eq. (33) and, then, computing the square of the absolute values of both the sides of the so-transformed Eq. (33). This algebraic manipulations yield the following two scalar equations

$$R_1\cos\theta_4 - R_2\sin\theta_4 + \left(\frac{R_3 - 2\,a_{31}^2}{a_{41}}\right) = 0 \tag{35a}$$

$$R_1\cos\theta_3 - R_2\sin\theta_3 - \left(\frac{R_3 - 2\,a_{41}^2}{a_{31}}\right) = 0 \tag{35b}$$

where

$$R_1 = 2\,(a_{11} - a_{21}\cos\xi_1 + a_{51}\cos\xi_2); \quad R_2 = 2\,(a_{21}\sin\xi_1 - a_{51}\sin\xi_2); \tag{36a}$$

$$R_3 = a_{11}^2 + a_{21}^2 + a_{31}^2 + a_{41}^2 + a_{51}^2 + 2[a_{11}(a_{51}\cos\xi_2 - a_{21}\cos\xi_1) - a_{21}a_{51}\cos(\xi_2 - \xi_1)] \tag{36b}$$
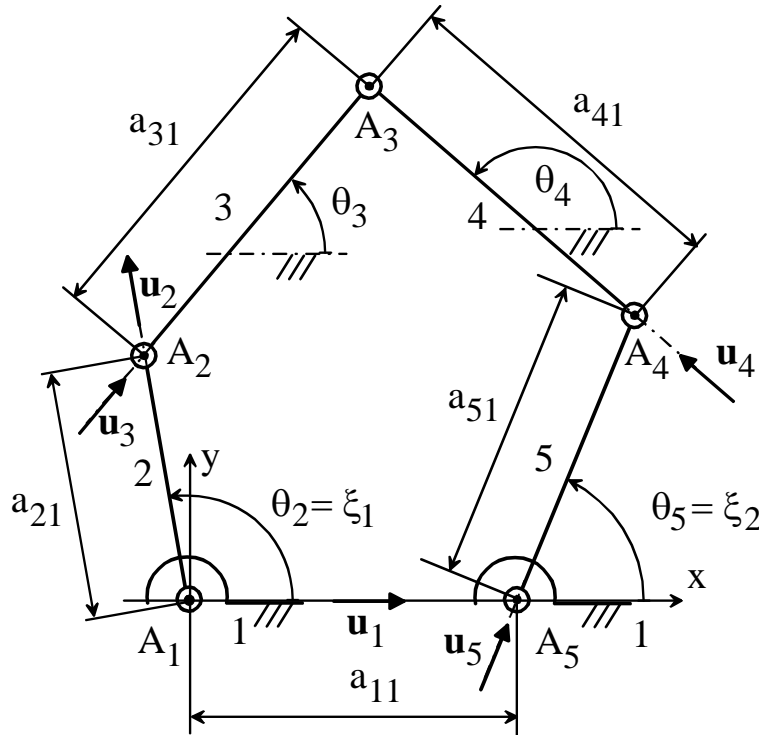

Figure 2: Five-bar linkage: kinematic scheme and notations

By exploiting the trigonometric identities $\cos x = [1 - \tan^2(x/2)]/[1 + \tan^2(x/2)]$ and $\sin x = 2\tan(x/2)/[1 + \tan^2(x/2)]$, Eqs. (35a) and (35b) become quadratic equations in $t_4 = \tan(\theta_4/2)$ and $t_3 = \tan(\theta_3/2)$, respectively, whose solutions yield

$$\theta_k = 2\tan^{-1}\left(\frac{R_2 \mp \sqrt{R_1^2 + R_2^2 - Q_k^2}}{Q_k - R_1}\right) \qquad k=3,4 \qquad (37)$$

with

$$Q_3 = -\left(\frac{R_3 - 2\,a_{41}^2}{a_{31}}\right); \qquad Q_4 = \left(\frac{R_3 - 2\,a_{31}^2}{a_{41}}\right) \qquad (38)$$

Equations (37) give the explicit expressions of the two secondary variables in the form of Eq. (1). Unfortunately, they do not provide pieces of information about how they are combined and it would seem that the PA has up to four solutions since there are up to two values of θ_3 and θ_4 for each value set of $\boldsymbol{\xi} = (\xi_1, \xi_2)^T$. Differently from this conclusion, Eq. (33) clearly shows that, if θ_4 (θ_3) is determined, for instance by solving Eq. (35a) (Eq. (35b)) through formula (37), θ_3 (θ_4) is uniquely determined through the unique expression of $\mathbf{z}_{31}$ (of $\mathbf{z}_{41}$), Eq. (33) provides, that is, $\mathbf{z}_{31} = \mathbf{z}_{11} + \mathbf{z}_{41} + \mathbf{z}_{51} - \mathbf{z}_{21}$ ($\mathbf{z}_{41} = \mathbf{z}_{21} + \mathbf{z}_{31} - \mathbf{z}_{11} - \mathbf{z}_{51}$). Thus, only two combinations of the values provided by Eq. (37) for θ_3 and θ_4 are valid solutions of the PA and the correct way of solving the PA is: i) use formula (37) for computing only one of the secondary variables, then ii) use Eq. (33) for computing the corresponding value of the other secondary variable. From a geometric point of view (see Fig. 2), once the generalized coordinates are assigned the position of the points A_2 and A_4 are assigned, too; and the up to two PA solutions correspond to the up to two possible positions of point A_3, which are given by the possible intersection points of two circles, one with center at A_2 and radius a_{31}, and the other with center at A_4 and radius a_{41}.

4.2. Velocity Analysis
Equation (26) when applied to Eq. (33) yields [$\mathbf{v}_1 = (0, 0)^T$; $\mathbf{v}_2 = (1, 0)^T$; $\mathbf{v}_5 = (0, 1)^T$; $\boldsymbol{\Lambda}_1 = \boldsymbol{\Lambda}_2 = \boldsymbol{\Lambda}_5 = \mathbf{0}_{2 \times 2}$]

$$\mathbf{D}_1(\boldsymbol{\xi}) = \mathbf{v}_2\,\mathbf{i}\,\mathbf{z}_{21} + \mathbf{v}_3\,\mathbf{i}\,\mathbf{z}_{31} - \mathbf{v}_4\,\mathbf{i}\,\mathbf{z}_{41} - \mathbf{v}_5\,\mathbf{i}\,\mathbf{z}_{51} \qquad (36)$$

where $\mathbf{v}_3 = (v_{31}, v_{32})^T = \nabla\theta_3$, and $\mathbf{v}_4 = (v_{41}, v_{42})^T = \nabla\theta_4$ are the unknowns.

Equating to zero (see Eq. (27a)) the vector expression of $\mathbf{D}_1$ given by formula (36) yields the following linear system of two decoupled complex equations with the same coefficients of the unknowns

$$v_{31}\,\mathbf{i}\,\mathbf{z}_{31} - v_{41}\,\mathbf{i}\,\mathbf{z}_{41} = -\,\mathbf{i}\,\mathbf{z}_{21} \qquad (37a)$$
$$v_{32}\,\mathbf{i}\,\mathbf{z}_{31} - v_{42}\,\mathbf{i}\,\mathbf{z}_{41} = \mathbf{i}\,\mathbf{z}_{51} \qquad (37b)$$

whose solutions are[12]

$$\mathbf{v}_3 = \frac{1}{a_{31}\sin(\theta_3 - \theta_4)}\begin{pmatrix} -a_{21}\sin(\theta_2 - \theta_4) \\ a_{51}\sin(\theta_5 - \theta_4) \end{pmatrix}; \quad \mathbf{v}_4 = \frac{1}{a_{41}\sin(\theta_3 - \theta_4)}\begin{pmatrix} -a_{21}\sin(\theta_2 - \theta_3) \\ a_{51}\sin(\theta_5 - \theta_3) \end{pmatrix}. \qquad (38)$$

By using the computed VCVs, the velocity of any point of the linkage can be analytically determined (see subsection 3.1). For instance, Eq. (28) applied to the path $A_1A_2A_3$ (Fig. 2) yields the following expression of $\mathbf{v}_{A_3|3}$

$$\mathbf{v}_{A_3|3} = \mathbf{v}_{A_2|3} + \mathbf{i}\,\dot{\boldsymbol{\xi}}^T\mathbf{v}_3\,\mathbf{z}_{31} \equiv \mathbf{i}\,\dot{\boldsymbol{\xi}}^T(\mathbf{v}_2\,\mathbf{z}_{21} + \mathbf{v}_3\,\mathbf{z}_{31}) \equiv \mathbf{i}\,\dot{\boldsymbol{\xi}}^T(\mathbf{v}_4\mathbf{i}\mathbf{z}_{41} + \mathbf{v}_5\mathbf{i}\mathbf{z}_{51})$$

where the velocity constraint of the R-pair in A_2 (i.e., $\mathbf{v}_{A_2|3} = \mathbf{v}_{A_2|2}(\equiv \mathbf{i}\,\dot{\boldsymbol{\xi}}^T\mathbf{v}_2\,\mathbf{z}_{21})$) has been used, and the last equality comes from the fact that $\mathbf{D}_1$ (i.e., the vector expression (36)) is equal to a null vector.

4.3. Acceleration Analysis
Equations (30a) and (30b) when applied to Eq. (33) yield [$\mathbf{v}_1 = (0, 0)^T$; $\mathbf{v}_2 = (1, 0)^T$; $\mathbf{v}_5 = (0, 1)^T$; $\boldsymbol{\Lambda}_1 = \boldsymbol{\Lambda}_2 = \boldsymbol{\Lambda}_5 = \mathbf{0}_{2 \times 2}$]

---

[12] It is worth reminding that the solution formulas of the complex equation $x\mathbf{a} + y\mathbf{b} = \mathbf{c}$, with x and y real unknowns and $\mathbf{a}$, $\mathbf{b}$ and $\mathbf{c}$ known complex coefficients, are ($\underline{\mathbf{z}}$ is the conjugate of $\mathbf{z}$)

$$x = \frac{\text{Im}(\mathbf{c}\underline{\mathbf{b}})}{\text{Im}(\mathbf{a}\underline{\mathbf{b}})}, \qquad y = \frac{\text{Im}(\mathbf{c}\underline{\mathbf{a}})}{\text{Im}(\mathbf{b}\underline{\mathbf{a}})}.$$

$$\mathbf{E}_1(\xi) = \Lambda_3\,\mathbf{i}\,\mathbf{z}_{31} - \Lambda_4\,\mathbf{i}\,\mathbf{z}_{41} \tag{39a}$$
$$\mathbf{F}_1(\xi) = \mathbf{v}_2\mathbf{v}_2^T\,\mathbf{i}\,\mathbf{z}_{21} + \mathbf{v}_3\mathbf{v}_3^T\,\mathbf{i}\,\mathbf{z}_{31} - \mathbf{v}_4\mathbf{v}_4^T\,\mathbf{i}\,\mathbf{z}_{41} - \mathbf{v}_5\mathbf{v}_5^T\,\mathbf{i}\,\mathbf{z}_{51} \tag{39b}$$

where the unknowns are six: the independent entries of $\Lambda_3 = \mathbf{H}(\theta_3)$ and $\Lambda_4 = \mathbf{H}(\theta_4)$, which will be denoted as follows

$$\Lambda_3 = \begin{bmatrix} \lambda_{31} & \lambda_{33} \\ \lambda_{33} & \lambda_{32} \end{bmatrix}; \quad \Lambda_4 = \begin{bmatrix} \lambda_{41} & \lambda_{43} \\ \lambda_{43} & \lambda_{42} \end{bmatrix}.$$

According to matrix expressions (39), equating $\mathbf{E}_1$ to $\mathbf{F}_1$ (see Eq. (31a)) yields the following linear system of three decoupled complex equations with the same coefficients of the unknowns

$$\lambda_{31}\,\mathbf{i}\,\mathbf{z}_{31} - \lambda_{41}\,\mathbf{i}\,\mathbf{z}_{41} = \mathbf{i}\,\mathbf{z}_{21} + v_{31}^2\,\mathbf{i}\,\mathbf{z}_{31} - v_{41}^2\,\mathbf{i}\,\mathbf{z}_{41} \tag{40a}$$
$$\lambda_{32}\,\mathbf{i}\,\mathbf{z}_{31} - \lambda_{42}\,\mathbf{i}\,\mathbf{z}_{41} = v_{32}^2\,\mathbf{i}\,\mathbf{z}_{31} - v_{42}^2\,\mathbf{i}\,\mathbf{z}_{41} - \mathbf{i}\,\mathbf{z}_{51} \tag{40b}$$
$$\lambda_{33}\,\mathbf{i}\,\mathbf{z}_{31} - \lambda_{43}\,\mathbf{i}\,\mathbf{z}_{41} = v_{31}v_{32}\,\mathbf{i}\,\mathbf{z}_{31} - v_{41}v_{42}\,\mathbf{i}\,\mathbf{z}_{41} \tag{40c}$$

whose solutions are

$$\Lambda_3 = \begin{bmatrix} v_{31}(v_{31}-1) & v_{31}v_{32} \\ v_{31}v_{32} & v_{32}(v_{32}-1) \end{bmatrix}; \quad \Lambda_4 = \begin{bmatrix} v_{41}(v_{41}-1) & v_{41}v_{42} \\ v_{41}v_{42} & v_{42}(v_{42}-1) \end{bmatrix}. \tag{41}$$

where the explicit expressions of v_{kj}, $k=3,4$ and $j=1,2$, are given by formulas (38).

By using the computed VCVs and ACJs, the acceleration of any point of the linkage can be analytically determined (see subsection 3.2). For instance, Eq. (32) applied to the path $A_1A_2A_3$ (Fig. 2) yields the following expression of $\mathbf{a}_{A_3|3}$

$$\mathbf{a}_{A_3|3} = \mathbf{a}_{A_2|3} + [\ddot{\xi}^T\mathbf{v}_3\mathbf{i} + \dot{\xi}^T(\Lambda_3\mathbf{i} - \mathbf{v}_3\mathbf{v}_3^T)\dot{\xi}]\mathbf{z}_{31} = (\ddot{\xi}_1\mathbf{i} - \dot{\xi}_1^2)\mathbf{z}_{21} + [\ddot{\xi}^T\mathbf{v}_3\mathbf{i} + \dot{\xi}^T(\Lambda_3\mathbf{i} - \mathbf{v}_3\mathbf{v}_3^T)\dot{\xi}]\mathbf{z}_{31}$$

where the acceleration constraint of the R-pair in A_2 (i.e., $\mathbf{a}_{A_2|3} = \mathbf{a}_{A_2|2}(\equiv(\ddot{\xi}_1\mathbf{i} - \dot{\xi}_1^2)\mathbf{z}_{21})$) has been used.

4.4. Singularity Analysis

The analysis of formulas (38) reveals that

a) $\mathbf{v}_3$ is a null vector (i.e., link 3 is at a stationary point (Eq. (7)) when $\theta_2 = \theta_4 \pm n\pi = \theta_5$ with $n=0,1$, that is, when links 4 and 5 are aligned (i.e., fully extended or folded) and link 2 is parallel to the aligned links 4 and 5 (Fig. 3);
b) $\mathbf{v}_4$ is a null vector (i.e., link 4 is at a stationary point (Eq. (7)) when $\theta_2 = \theta_3 \pm n\pi = \theta_5$ with $n=0,1$, that is, when links 2 and 3 are aligned (i.e., fully extended or folded) and link 5 is parallel to the aligned links 2 and 3 (Fig. 4);
c) the zeroing of any coefficient $(1/v_{kj})$, for $k=3,4$, and $j=1,2$, occurs (i.e., the input links are at a stationary point) if and only if $\theta_3 = \theta_4 \pm n\pi$ with $n=0,1$, that is, the two input links (i.e., links 2 and 5) simultaneously are at a stationary point when the two output links (i.e., links 3 and 4) are aligned (i.e., fully extended or folded) (Fig.5).

Regarding conditions a) and b), in this case, since the ACJs are null matrices (see Eq. (41)) when the corresponding VCVs are null vectors, the ACJs are not able to clarify [30] whether these stationary points are extreme poses of the output links they refer to, and the direct comparison is necessary. Such comparison (see Figs. 3 and 4) shows that they are indeed.

Regarding condition c), the found geometric condition corresponds to the coincidence of the two PA solutions. Also, it states the following analytic relationship between the two generalized coordinates, ξ_1 and ξ_2,

$$(a_{31} \pm a_{41})^2 = (a_{21}\cos\xi_1 - a_{11} - a_{51}\cos\xi_2)^2 + (a_{21}\sin\xi_1 - a_{51}\sin\xi_2)^2 \tag{42}$$

All the configurations that satisfy Eq. (42) are singular. So, there are infinite mechanism configurations that satisfy condition c), and the ones shown in Fig. 5 are only two of many.

For the studied linkage, finding the configurations where each v_{kj}, for $k=3,4$, and $j=1,2$, is equal to zero could be of interest since they identify the extreme positions the k-th output link can reach by changing the j-th input variable while the other input is kept locked. The analysis of formulas (38) reveals that

- v_{31} is equal to zero when links 2 and 4 are parallel to one another;
- v_{32} is equal to zero when links 4 and 5 are aligned (i.e., fully extended or folded);
- v_{41} is equal to zero when links 2 and 3 are aligned (i.e., fully extended or folded);
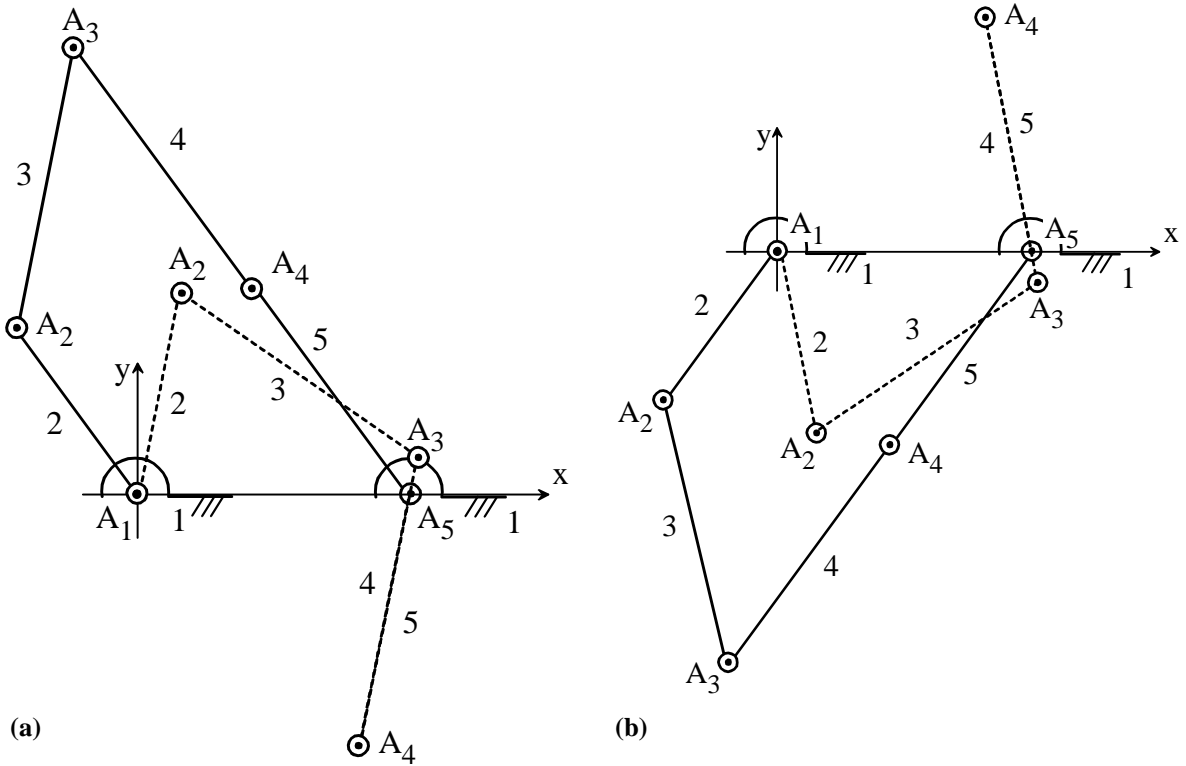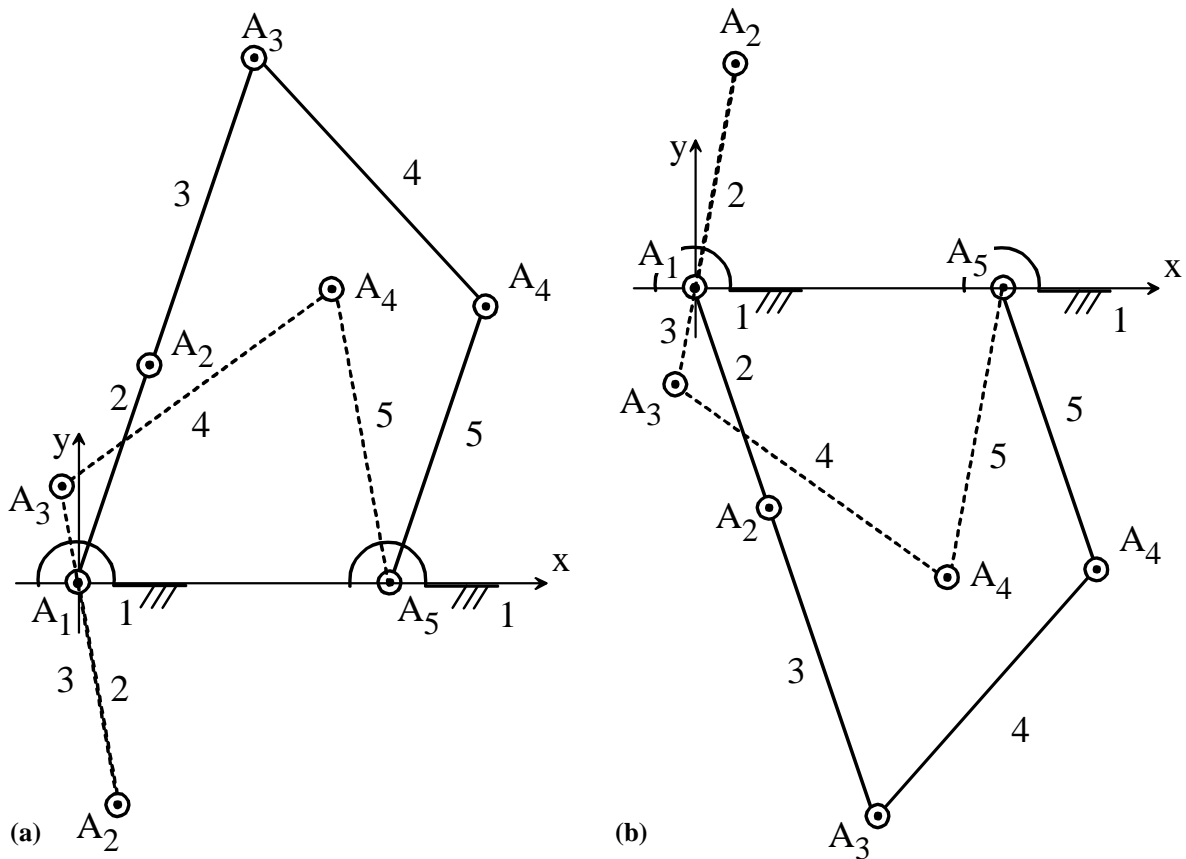- v_{42} is equal to zero when links 5 and 3 are parallel to one another.

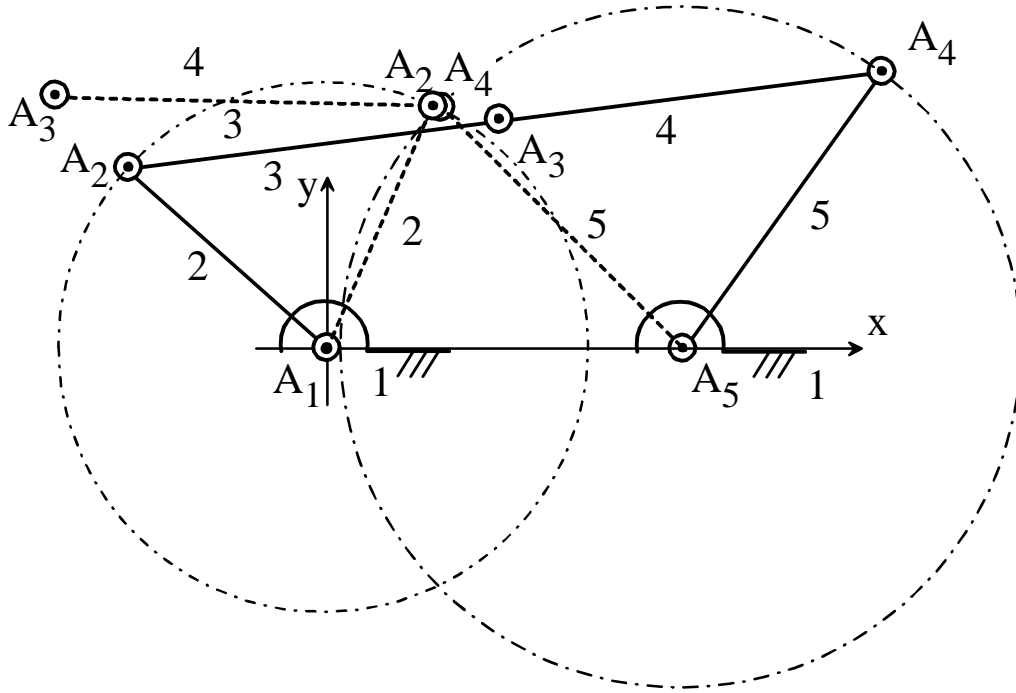**Figure 3:** Five-bar linkage with $(a_{11}/a_{21})=1.34$, $(a_{31}/a_{21})=1.43$, $(a_{41}/a_{21})=1.45$, and $(a_{51}/a_{21})=1.29$: extreme poses of link 3, (a) for the path branch with A_3 at the right-hand side of the vector $(\mathbf{A}_2 - \mathbf{A}_4)$ (i.e., the one corresponding to the 1st PA solution), and (b) for the path branch with A_3 at the left-hand side of the vector $(\mathbf{A}_2 - \mathbf{A}_4)$ (i.e., the one corresponding to the 2nd PA solution).

Figure 4: Five-bar linkage with $(a_{11}/a_{21})=1.34$, $(a_{31}/a_{21})=1.43$, $(a_{41}/a_{21})=1.45$, and $(a_{51}/a_{21})=1.29$: extreme poses of link 4, (a) for the path branch with A_3 at the right-hand side of the vector $(\mathbf{A}_2 - \mathbf{A}_4)$ (i.e., the one corresponding to the 1st PA solution), and (b) for the path branch with A_3 at the left-hand side of the vector $(\mathbf{A}_2 - \mathbf{A}_4)$ (i.e., the one corresponding to the 2nd PA solution).

13

Figure 5: Five-bar linkage with $(a_{11}/a_{21})=1.34$, $(a_{31}/a_{21})=1.43$, $(a_{41}/a_{21})=1.45$, and $(a_{51}/a_{21})=1.29$: two stationary points of the input links (i.e., two configurations that satisfy Eq. (42)), one with links 3 and 4 fully extended and the other with links 3 and 4 fully folded.

The above-identified singularities concur with what is reported in the literature [31–34] by using other singularity-analysis techniques.

5. Conclusions

The novel concepts of velocity-coefficient vector (VCV) and acceleration-coefficient Jacobian (ACJ) have been presented for multi-DOF scleronomic and holonomic mechanisms, and it has been proved that VCV and ACJ are the correct extensions of the concepts of velocity coefficient (VC) and acceleration coefficient (AC), respectively, which, in the literature, have been presented for single-DOF planar mechanisms.

In particular, VCVs and ACJs depend only on the mechanism configurations, and they are effective in solving mechanisms' kinematic analysis and in identifying mechanism singularities; the same as VCs and ACs do for single-DOF planar mechanisms. Eventually, they become VCs and ACs, respectively, when applied to single-DOF mechanisms.

A novel algorithm that solves all the kinematic-analysis problems and the singularity analysis has been proposed for planar multi-DOF mechanisms. This algorithm is based on the systematic use of VCVs and ACJs and adopts a notation, based on the complex-number method, which the author has previously presented for single-DOF planar mechanisms.

The proposed algorithm computes one VCV and one ACJ for each mobile link of the mechanism by sequentially solving linear systems automatically writable from the mechanism constraint equations; then, it uses the computed VCVs and ACJs for determining the velocity and/or the acceleration of any point of the mechanism, and for finding all its singular configurations.

The numerical efficiency of the proposed algorithm stands on the fact that the coefficients of the unknowns that appear in the linear systems to solve are the same and that the unknowns' coefficient matrix is sparse and, often, reducible to decoupled sub-matrices. The automatic deduction of the equations to solve makes the proposed algorithm suitable for general purpose programs conceived to constitute the kinematic block of any multi-body simulation environment devoted to planar mechanisms. Also, the algorithm is simple enough for being presented in graduate courses since its theoretical basis are multivariable calculus and complex numbers, which belong to the mathematical background of graduate students. All these qualities have been verified by applying it to a relevant case study.

References

1. Marghitu, D.B.: Mechanisms and Robots Analysis with MATLAB. Springer-Verlag, London, (2009).
2. Galletti, C.U.: A Note on Modular Approaches to Planar Linkage Kinematic Analysis. Mech. Mach. Theory 21(5), 385-391 (1986).
3. Bràt, V., Lederer, P.: KIDYAN: Computer-Aided Kinematic and Dynamic Analysis of Planar Mechanisms. Mech. Mach. Theory 8, 457-467 (1973).
4. Nikravesh, P.E.: Planar Multibody Dynamics. CRC Press, Boca Raton FL (2018).
5. Wampler, C.: Solving the Kinematics of Planar Mechanisms. J. Mech. Des 121(3), 387-391 (1999).
6. Wampler, C.: Solving the Kinematics of Planar Mechanisms by Dixon Determinant and a Complex-Plane Formulation. J. Mech. Des 123(3), 382-387 (2001).
7. Kleiner, I.: Thinking the Unthinkable: the Story of Complex Numbers (with a Moral). Mathematics Teacher 81, 583-592 (Oct., 1988).
8. Zwikker, C.: The Advanced Geometry of Plane Curves and Their Applications. Dover Publications, Inc., New York USA (1963, reprint of "Advanced Plane Geometry" published in 1950).
9. Luck, K., Modler, K.-H.: Getriebetechnik. Analyse, Synthese und Optimierung. 2nd Ed. Springer-Verlag, Berlin DE (1995).
10. Dijksman, E. A.: Motion Geometry of Mechanisms. Cambridge University Press, Cambridge UK (1976)
11. Paul, B.: Kinematics and Dynamics of Planar Machinary. Prentice-Hall, Inc., Englewood Cliffs N.J. (1987).
12. Haug, E.J.: Computer Aided Kinematics and Dynamics of Mechanical Systems. Allyn and Bacon, Needham Heights MA (1989).
13. Di Gregorio, R.: Systematic use of velocity and acceleration coefficients in the kinematic analysis of single-DOF planar mechanisms. Mech. Mach. Theory 139(September 2019), 310-328 (2019).
14. Rothbart, H.A.: Cam Design Handbook. McGraw-Hill,Inc., New York NY (2004).
15. Norton, R.L., Cam Design and Manufacturing Handbook, 2nd Ed. Industrial Press, New York NY (2009).
16. Litvin, F.L., Fuentes-Aznar, A., Gonzalez-Perez, I., Hayasaka, K.: Noncircular Gears: Design and Generation. Cambridge University Press, Cambridge UK (2009).
17. Barton, L.O.: Mechanism Analysis, Simplified and Graphical Techniques, 2nd Ed. CRC Press, Boca Raton FL (1993).
18. Uicker, J.J., Pennock, G. R., Shigley, J.E.: Theory of Machines and Mechanisms, 3rd Ed. Oxford University Press, Oxford UK (2003).
19. Goodman, T.P.: An indirect method for determining accelerations in complex mechanisms. Trans. ASME, Vol. 81, November 1958, ASME Paper No. 57-A-108, pp. 1676-1682 (1958).
20. Modrey, J.: Analysis of Complex Kinematic Chains with Influence Coefficients. J. Appl. Mechanics, vol 26; Trans. ASME, Vol. 81 ser. E, June 1959, pp. 184-188 (1959).
21. Goodman T.P., Hall A.S.: Discussion on "Analysis of Complex Kinematic Chains with Influence Coefficients" by Modrey. J. Appl. Mechanics, Vol. 27, March 1960, pp. 215-216 (1960).
22. Di Gregorio, R.: An Algorithm for Analytically Calculating the Positions of the Secondary Instant Centers of Indeterminate Linkages. J. Mech. Des 130(4), 042303-(1-9) (2008).
23. Di Gregorio, R.: A novel dynamic model for single-degree-of-freedom planar mechanisms based on instant centers. ASME J. of Mechanisms and Robotics 8(1), 011013-(8pages) (2016).
24. Di Gregorio, R.: On the Use of Instant Centers to Build Dynamic Models of Single-dof Planar Mechanisms. In: Lenarcic J., Parenti-Castelli V. (eds) Advances in Robot Kinematics 2018. Springer Proceedings in Advanced Robotics, vol 8, pp. 242-249. Springer, Cham (2018).
25. Di Gregorio, R.: A novel geometric and analytic technique for the singularity analysis of one-dof planar mechanisms. Mech. Mach. Theory, 42(11), 1462-1483, (2007).
26. Gosselin, C.M., Angeles, J.: Singularity analysis of closed-loop kinematic chains. IEEE Trans. Robot. Automat., 6 (3), 281–290, (1990).
27. Ma, O., Angeles, J.: Architecture singularities of platform manipulators. Proceedings of the 1991 IEEE International Conference on Robotics and Automation, Sacramento (CA, USA), pp. 1542–1547, (1991).
28. Zlatanov, D., Fenton, R.G., Benhabib, B.: A unifying framework for classification and interpretation of mechanism singularities. ASME J. Mech. Des., 117 (4), 566–572, (1995).
29. Hunt, K.H.: Kinematic Geometry of Mechanisms, Oxford University Press, Oxford UK (1978), ISBN: 0-19-856124-5.
30. Adams R., Essex C.: Calculus: a complete course, 7th Ed. Pearson, Toronto CAN (2019).

31. Theingi, Li C., Chen I-M., Angeles J.: Singularity Management of 2DOF Planar Manipulator Using Coupled Kinematics. Proceedings of the 7th International Conference on Control, Automation, Robotics and Vision (ICARCV'O2), Dec. 2002, Singapore, pp. 402–407.

32. Li C., Theingi, Chen I-M.: Cases Study on the Singularity of Five-Bar Planar Mechanism with Differential Gear Drives. In H. R. Parsaei, M. Gen, H. R. Leep, J. P. Wong (Eds.), Proceedings of the 6th International Conference on Engineering Design and Automation, Aug. 4-7, 2002, Maui (Hawaii, USA), pp. 399–404, (2002).

33. Six D., Briot S., Chriette A., Martinet P.: A Controller Avoiding Dynamic Model Degeneracy of Parallel Robots during Singularity Crossing. ASME J. of Mechanisms and Robotics, American Society of Mechanical Engineers, 9(5), 051008 (8 pages), (Aug 07, 2017).

34. Yuan X.-F., Zhou L., Duan Y.-F.: Singularity and kinematic bifurcation analysis of pin-bar mechanisms using analogous stiffness method. International Journal of Solids and Structures, 49(10), 1212–1226, (2012)

Appendix

In this appendix the demonstration that the matrices $\mathbf{G}_{Rc|i}$ and $\mathbf{G}_{Sc|n}$ are symmetric is reported. According to Eqs. (19a) the following relationships hold:

$$\frac{\partial \mathbf{L}_{Rc|i}}{\partial \psi_{i1}} = \frac{\partial^2 \mathbf{z}_{Rc|i}}{\partial \psi_{i1}^2} \boldsymbol{\varepsilon}_{i1} + \frac{\partial^2 \mathbf{z}_{Rc|i}}{\partial \psi_{i2} \partial \psi_{i1}} \boldsymbol{\varepsilon}_{i2} + \frac{\partial^2 \mathbf{z}_{Rc|i}}{\partial \theta_{i1} \partial \psi_{i1}} \mathbf{v}_{i1} + \frac{\partial^2 \mathbf{z}_{Rc|i}}{\partial \theta_{i2} \partial \psi_{i1}} \mathbf{v}_{i2} \tag{A.1a}$$

$$\frac{\partial \mathbf{L}_{Rc|i}}{\partial \psi_{i2}} = \frac{\partial^2 \mathbf{z}_{Rc|i}}{\partial \psi_{i2} \partial \psi_{i1}} \boldsymbol{\varepsilon}_{i1} + \frac{\partial^2 \mathbf{z}_{Rc|i}}{\partial \psi_{i2}^2} \boldsymbol{\varepsilon}_{i2} + \frac{\partial^2 \mathbf{z}_{Rc|i}}{\partial \theta_{i1} \partial \psi_{i2}} \mathbf{v}_{i1} + \frac{\partial^2 \mathbf{z}_{Rc|i}}{\partial \theta_{i2} \partial \psi_{i2}} \mathbf{v}_{i2} \tag{A1.b}$$

$$\frac{\partial \mathbf{L}_{Rc|i}}{\partial \theta_{i1}} = \frac{\partial^2 \mathbf{z}_{Rc|i}}{\partial \theta_{i1} \partial \psi_{i1}} \boldsymbol{\varepsilon}_{i1} + \frac{\partial^2 \mathbf{z}_{Rc|i}}{\partial \psi_{i2} \partial \theta_{i1}} \boldsymbol{\varepsilon}_{i2} + \frac{\partial^2 \mathbf{z}_{Rc|i}}{\partial \theta_{i1}^2} \mathbf{v}_{i1} + \frac{\partial^2 \mathbf{z}_{Rc|i}}{\partial \theta_{i2} \partial \theta_{i1}} \mathbf{v}_{i2} \tag{A1.c}$$

$$\frac{\partial \mathbf{L}_{Rc|i}}{\partial \theta_{i2}} = \frac{\partial^2 \mathbf{z}_{Rc|i}}{\partial \theta_{i2} \partial \psi_{i1}} \boldsymbol{\varepsilon}_{i1} + \frac{\partial^2 \mathbf{z}_{Rc|i}}{\partial \psi_{i2} \partial \theta_{i2}} \boldsymbol{\varepsilon}_{i2} + \frac{\partial^2 \mathbf{z}_{Rc|i}}{\partial \theta_{i1} \partial \theta_{i2}} \mathbf{v}_{i1} + \frac{\partial^2 \mathbf{z}_{Rc|i}}{\partial \theta_{i2}^2} \mathbf{v}_{i2} \tag{A1.d}$$

The introduction of Eqs. (A1) into the expression of $\mathbf{G}_{Rc|i}$ given by Eqs. (19c) yields

$$\mathbf{G}_{Rc|i} = \frac{\partial^2 \mathbf{z}_{Rc|i}}{\partial \psi_{i1}^2} \boldsymbol{\varepsilon}_{i1} \boldsymbol{\varepsilon}_{i1}^T + \frac{\partial^2 \mathbf{z}_{Rc|i}}{\partial \psi_{i2}^2} \boldsymbol{\varepsilon}_{i2} \boldsymbol{\varepsilon}_{i2}^T + \frac{\partial^2 \mathbf{z}_{Rc|i}}{\partial \theta_{i1}^2} \mathbf{v}_{i1} \mathbf{v}_{i1}^T + \frac{\partial^2 \mathbf{z}_{Rc|i}}{\partial \theta_{i2}^2} \mathbf{v}_{i2} \mathbf{v}_{i2}^T + \frac{\partial^2 \mathbf{z}_{Rc|i}}{\partial \psi_{i2} \partial \psi_{i1}} (\boldsymbol{\varepsilon}_{i2} \boldsymbol{\varepsilon}_{i1}^T + \boldsymbol{\varepsilon}_{i1} \boldsymbol{\varepsilon}_{i2}^T) + \frac{\partial^2 \mathbf{z}_{Rc|i}}{\partial \theta_{i1} \partial \psi_{i1}} (\mathbf{v}_{i1} \boldsymbol{\varepsilon}_{i1}^T + \boldsymbol{\varepsilon}_{i1} \mathbf{v}_{i1}^T) +$$
$$+ \frac{\partial^2 \mathbf{z}_{Rc|i}}{\partial \theta_{i1} \partial \psi_{i2}} (\mathbf{v}_{i1} \boldsymbol{\varepsilon}_{i2}^T + \boldsymbol{\varepsilon}_{i2} \mathbf{v}_{i1}^T) + \frac{\partial^2 \mathbf{z}_{Rc|i}}{\partial \theta_{i2} \partial \psi_{i1}} (\mathbf{v}_{i2} \boldsymbol{\varepsilon}_{i1}^T + \boldsymbol{\varepsilon}_{i1} \mathbf{v}_{i2}^T) + \frac{\partial^2 \mathbf{z}_{Rc|i}}{\partial \theta_{i2} \partial \psi_{i2}} (\mathbf{v}_{i2} \boldsymbol{\varepsilon}_{i2}^T + \boldsymbol{\varepsilon}_{i2} \mathbf{v}_{i2}^T) + \frac{\partial^2 \mathbf{z}_{Rc|i}}{\partial \theta_{i2} \partial \theta_{i1}} (\mathbf{v}_{i2} \mathbf{v}_{i1}^T + \mathbf{v}_{i1} \mathbf{v}_{i2}^T)$$
$$\tag{A2}$$

The analysis of Eq. (A2) reveals that the matrix $\mathbf{G}_{Rc|i}$ is a linear combination of symmetric matrices with complex coefficients. This brings to conclude that $\mathbf{G}_{Rc|i}$ is a symmetric matrix. Also, since the expression of $\mathbf{G}_{Sc|n}$ given by Eqs. (19c) is obtained from the one of $\mathbf{G}_{Rc|i}$ by replacing the right subscripts Rc and i with Sc and n, respectively, the same conclusion holds for the matrix $\mathbf{G}_{Sc|n}$. *QED*

Figure Captions

Figure 1: Notations introduced in [13]: k-th link, traversed by q independent loops, in contact with the w-th link at A_{p+i} through an higher pair, and containing the linear guide of a P-pair that connects it to a slider fixed in the s-th link.

Figure 2: Five-bar linkage: kinematic scheme and notations.

Figure 3: Five-bar linkage with $(a_{11}/a_{21})=1.34$, $(a_{31}/a_{21})=1.43$, $(a_{41}/a_{21})=1.45$, and $(a_{51}/a_{21})=1.29$: extreme poses of link 3, (a) for the path branch with A_3 at the right-hand side of the vector $(\mathbf{A}_2 - \mathbf{A}_4)$ (i.e., the one corresponding to the 1st PA solution), and (b) for the path branch with A_3 at the left-hand side of the vector $(\mathbf{A}_2 - \mathbf{A}_4)$ (i.e., the one corresponding to the 2nd PA solution).

Figure 4: Five-bar linkage with $(a_{11}/a_{21})=1.34$, $(a_{31}/a_{21})=1.43$, $(a_{41}/a_{21})=1.45$, and $(a_{51}/a_{21})=1.29$: extreme poses of link 4, (a) for the path branch with A_3 at the right-hand side of the vector $(\mathbf{A}_2 - \mathbf{A}_4)$ (i.e., the one corresponding to the 1st PA solution), and (b) for the path branch with A_3 at the left-hand side of the vector $(\mathbf{A}_2 - \mathbf{A}_4)$ (i.e., the one corresponding to the 2nd PA solution).

Figure 5: Five-bar linkage with $(a_{11}/a_{21})=1.34$, $(a_{31}/a_{21})=1.43$, $(a_{41}/a_{21})=1.45$, and $(a_{51}/a_{21})=1.29$: two stationary points of the input links (i.e., two configurations that satisfy Eq. (42)), one with links 3 and 4 fully extended and the other with links 3 and 4 fully folded.
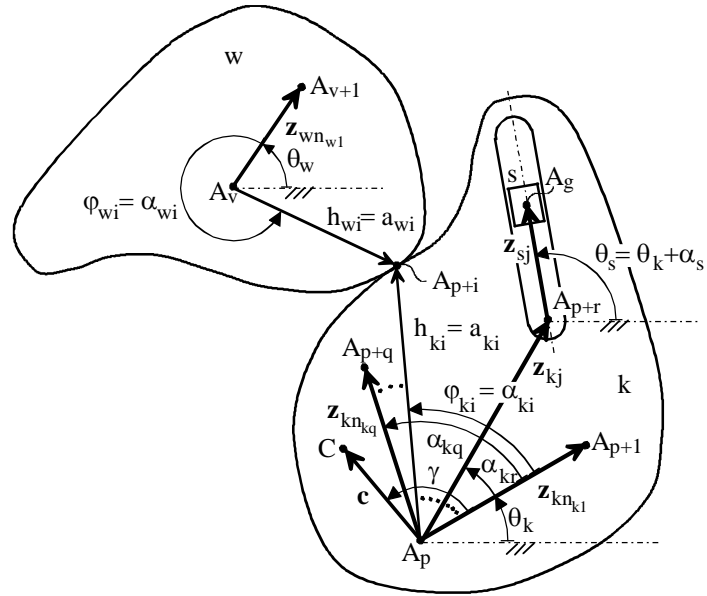
Figure 1: Notations introduced in [13]: k-th link, traversed by q independent loops, in contact with the w-th link at A_{p+i} through an higher pair, and containing the linear guide of a P-pair that connects it to a slider fixed in the s-th link.
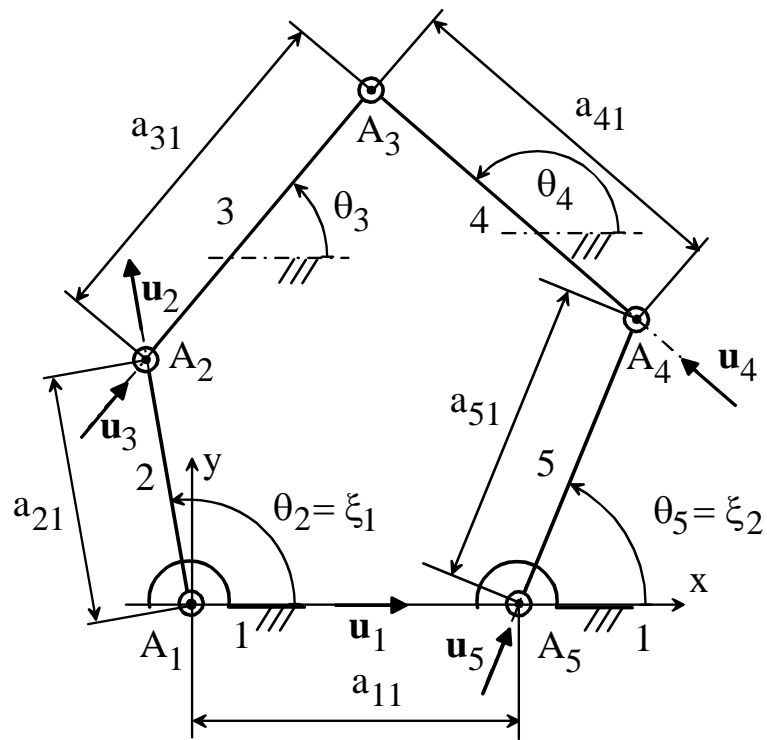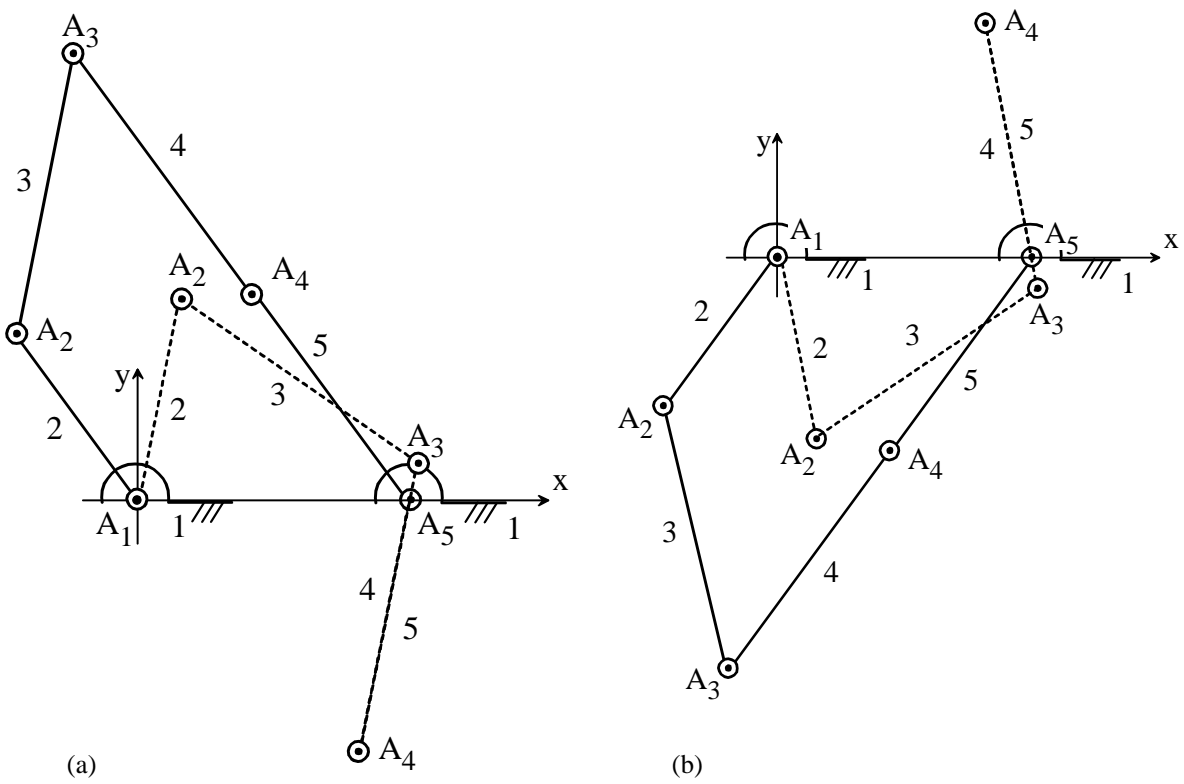
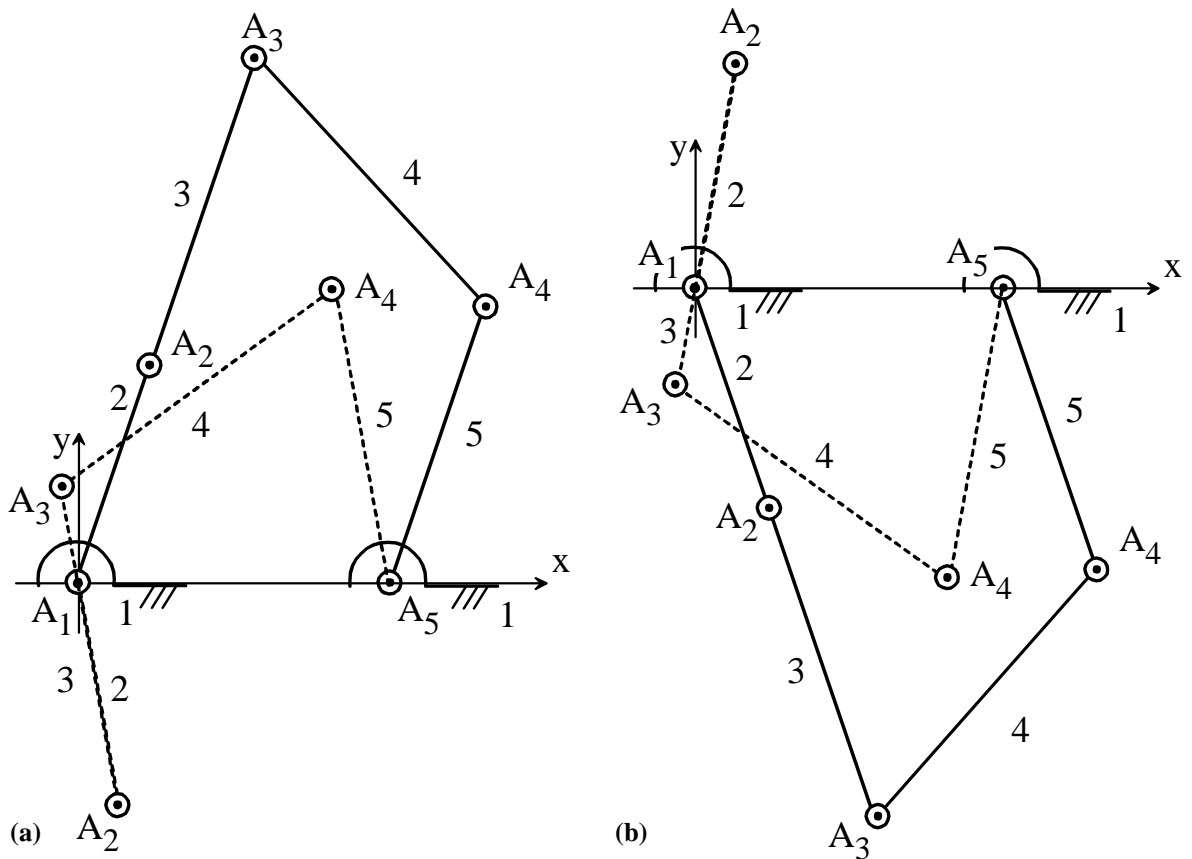**Figure 2:** Five-bar linkage: kinematic scheme and notations

Figure 3: Five-bar linkage with $(a_{11}/a_{21})=1.34$, $(a_{31}/a_{21})=1.43$, $(a_{41}/a_{21})=1.45$, and $(a_{51}/a_{21})=1.29$: extreme poses of link 3, (a) for the path branch with A_3 at the right-hand side of the vector $(A_2 - A_4)$ (i.e., the one corresponding to the 1st PA solution), and (b) for the path branch with A_3 at the left-hand side of the vector $(A_2 - A_4)$ (i.e., the one corresponding to the 2nd PA solution).

Figure 4: Five-bar linkage with $(a_{11}/a_{21})=1.34$, $(a_{31}/a_{21})=1.43$, $(a_{41}/a_{21})=1.45$, and $(a_{51}/a_{21})=1.29$: extreme poses of link 4, (a) for the path branch with A_3 at the right-hand side of the vector $(\mathbf{A}_2 - \mathbf{A}_4)$ (i.e., the one corresponding to the 1st PA solution), and (b) for the path branch with A_3 at the left-hand side of the vector $(\mathbf{A}_2 - \mathbf{A}_4)$ (i.e., the one corresponding to the 2nd PA solution).
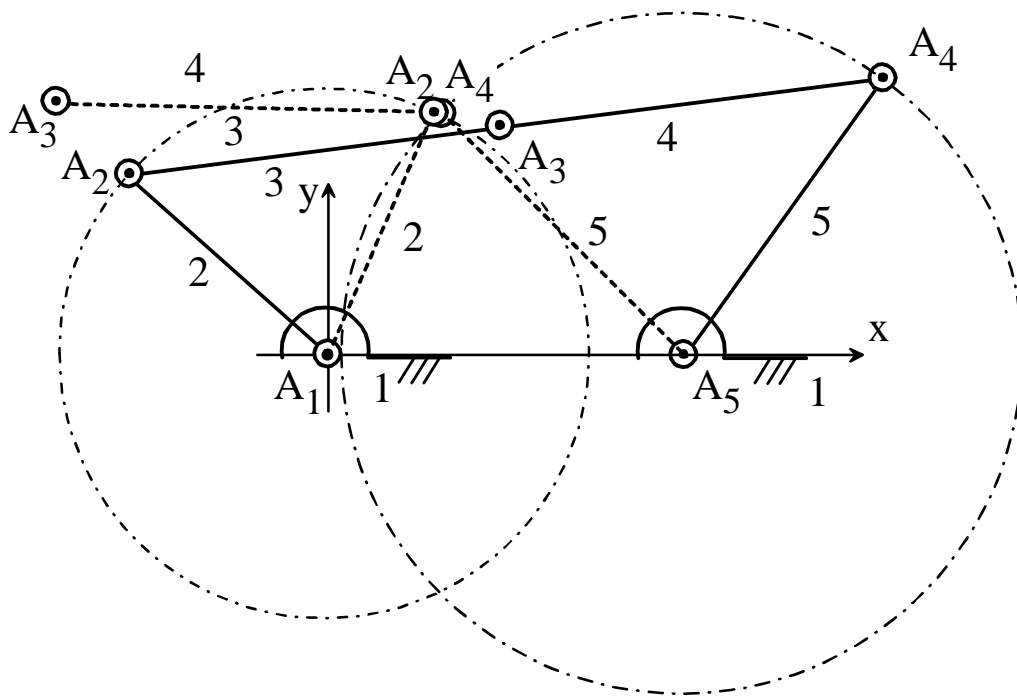
Figure 5: Five-bar linkage with $(a_{11}/a_{21})=1.34$, $(a_{31}/a_{21})=1.43$, $(a_{41}/a_{21})=1.45$, and $(a_{51}/a_{21})=1.29$: two stationary points of the input links (i.e., two configurations that satisfy Eq. (42)), one with links 3 and 4 fully extended and the other with links 3 and 4 fully folded.